cells showed membranous positive staining, and the results for NICD were considered positive when cells displayed nuclear staining. Two independent observers interpreted the immunohistochemical data in a blinded manner. For each specimen, one score was assigned according to the percentage of positive cells: <5%: 1 point; 6–35%: 2 points; 36–70%: 3 points; and >71%: 4 points, and another score was assigned according to the intensity of the staining, with negative staining equaling 1 point, weak staining equaling 2 points, moderate staining equaling 3 points and strong staining equaling 4 points. Notch1and JAG1 expression scores were then calculated by multiplying the two scores described above. If the expression score was ≥4, the tumor was considered to be positive.

Cell Lines

Human OSCC cell lines, namely, HSC-2, HSC-3, SAS, SCC-KN and Ca9-22 were kindly donated by the Department of Oral and Maxillofacial Surgery, Graduate School of Dental Science, Kyushu University and OSC-20, OSC-19 and HOC-313 were kindly donated by the Department of Oral and Maxillofacial Surgery, Kanazawa University Graduate School of Medical Science. All cell lines were cultured in Dulbecco's modified Eagle's medium (DMEM; GIBCO, Gland Island, NY, USA) with 10% fetal bovine serum (FBS). The cells were incubated at 37 °C in 5% CO_2 and saturated humidity.

Western Blotting

Cells were lysed on ice in 150 mM NaCl, 1% Triton X-100, 0.5% sodium deoxycholate, 0.1% SDS, 1 mM EDTA-2Na (pH 8.0), 1 mM EGTA (pH 7.5), 2.5 mM sodium pyrophosphate, 1 mM β-glycerophosphate, 1 mM Na_2VO_4, 1 mM PMSF and 20 mM Tris-HCl (pH 7.5) containing a protease inhibitor cocktail (Roche Diagnostics, Basel, Switzerland). Protein concentrations were determined using the BCA assay (Bio-Rad Laboratories, Hercules, CA, USA). Samples were boiled with Laemmli buffer. Equal amounts of protein were electrophoresed on polyacrylamide gels containing 0.1% SDS, transferred to PVDF membranes (Millipore, Hamburg, Germany) and incubated with specific primary antibodies against Notch1 rabbit monoclonal antibodies (C44H11; Cell Signaling Technology), cleaved Notch1 (Val1744) rabbit monoclonal antibodies (D3B8; Cell Signaling Technology), Hes1 rabbit antibodies (a kind gift from Dr Sudo, Toray Corporation, Yokohama, Japan),[26] Hes related with YRPW motif 1 (Hey1) rabbit polyclonal antibodies (ab22614; Abcam, Cambridge, UK), Akt (Cell Signaling Technology), phosphorylated Akt (Ser473) murine monoclonal antibodies (p-Akt; 587F11; Cell Signaling Technology), phosphorylated histone H3 (p-H3; Ser10; Millipore) and β-actin (AC-74; Sigma Aldrich, St Louis, MO, USA). Proteins of interest were detected with appropriate horseradish peroxidase-conjugated secondary antibodies and an enhanced chemiluminescence substrate (Amersham Pharmacia Biotech, Buckinghamshire, UK).

RNA Isolation, RT-PCR and Quantitative Real-Time PCR

Total RNA was isolated using Trizol (Invitrogen, Carlsbad, CA, USA) according to the instructions provided by the manufacturer and reverse transcribed into cDNA using SuperscriptIII (Invitrogen) and oligo (dT). For qualitative PCR, the cDNA was amplified using PCR with specific primers. The following primers were used: *Notch1* (forward: 5′-CGGGACATCACGGATCATATGGAC-3′; reverse: 5′-CCA CCCAGCGCCGCCATCTCGGGC-3′); *JAG1* (forward: 5′-CG GGATTTGGTTAATGGTTATC-3′; reverse: 5′-ATAGTCACTG GCACGGTTGTAGCAC-3′); *Hes1* (forward: 5′-TGGAAATG ACAGTGAAGCACCTC-3′; reverse: 5′-TCGTTCATGCACTC GCTGAAG-3′); *Hey1* (forward: 5′-CGAGGTGGAGAAGGAG AGTG-3′; reverse: 5′-CTGGGTACCAGCCTTCTCAG-3′); and *β-actin* (forward: 5′-GTGGGGCGCCCCAGGCACCA-3′; reverse: 5′-CTCCTTAATGTCACGCACGATTTC-3′). The PCR products were analyzed using agarose gel electrophoresis and visualized using staining with ethidium bromide.

For quantitative real-time PCR (qRT-PCR), each reaction mixture was diluted fivefold with DNase/RNase-free water (Invitrogen), and 4 μl of each mixture were subjected to PCR. The reactions were run using THUNDERBIRD SYBR qPCR Mix (Toyobo, Osaka, Japan) on a Light Cycler 1.5 (Roche, Indianapolis, IN, USA). The comparative Ct (ΔΔCt) method was used to determine fold changes in expression using glyceraldehyde-3-phosphate dehydrogenase (GAPDH). Each sample was run in triplicate. The following primers were used: *Snail* (forward: 5′-TCGGAAGCCTAAACTACAGCGA-3′; reverse: 5′-AGATGAGCATTGGCAGCGAG-3′); *Slug* (forward: 5′-AAGCATTTCAACGCCTCCAAA-3′; reverse: 5′-GGATCTC TGGTTGTGGTATGACA-3′); *Twist* (forward: 5′-GTCCGCAG TCTTACGAGGAG-3′; reverse: 5′-GCTTGAGGGTCTGAATC TTGCT-3′); and *GAPDH* (forward: 5′-TGTTGCCATCAATG ACCCCTT-3′; reverse: 5′-CTCCACGACGTACTCAGCG-3′). The cycling conditions were as follows: initial denaturation at 98 °C for 5 min, followed by 45 cycles at 98 °C for 15 s, 60 °C for 30 s and 72 °C for 60 s. The experiments were performed in triplicate.

Immunofluorescence Microscopy

The cells were fixed in 4% paraformaldehyde in a phosphate-buffered saline (PBS) solution for 30 min. After fixation was completed, the cells were centrifuged at 2500 r.p.m. for 10 to 15 min. The supernatant was poured off and the cell pellets were embedded in paraffin blocks. Microtome was used to section the blocks of FFPE cells into 4-μm-thick sections. The sections were then transferred to glass slides. The slides were deparaffinized before being analyzed. After being blocked with Protein Block Serum-Free Reagent (Dako) for 30 min, the primary antibodies were diluted in Dako Real™ Antibody Reagent (Dako). After being incubated for 24 h with the antibodies and subsequently washed with PBS three times (5 min each), the cells were incubated with the secondary antibodies (Alexa Fluor® 568 donkey anti-goat IgG; Molecular Probes, Eugene, OR, USA) diluted in Dako Real™

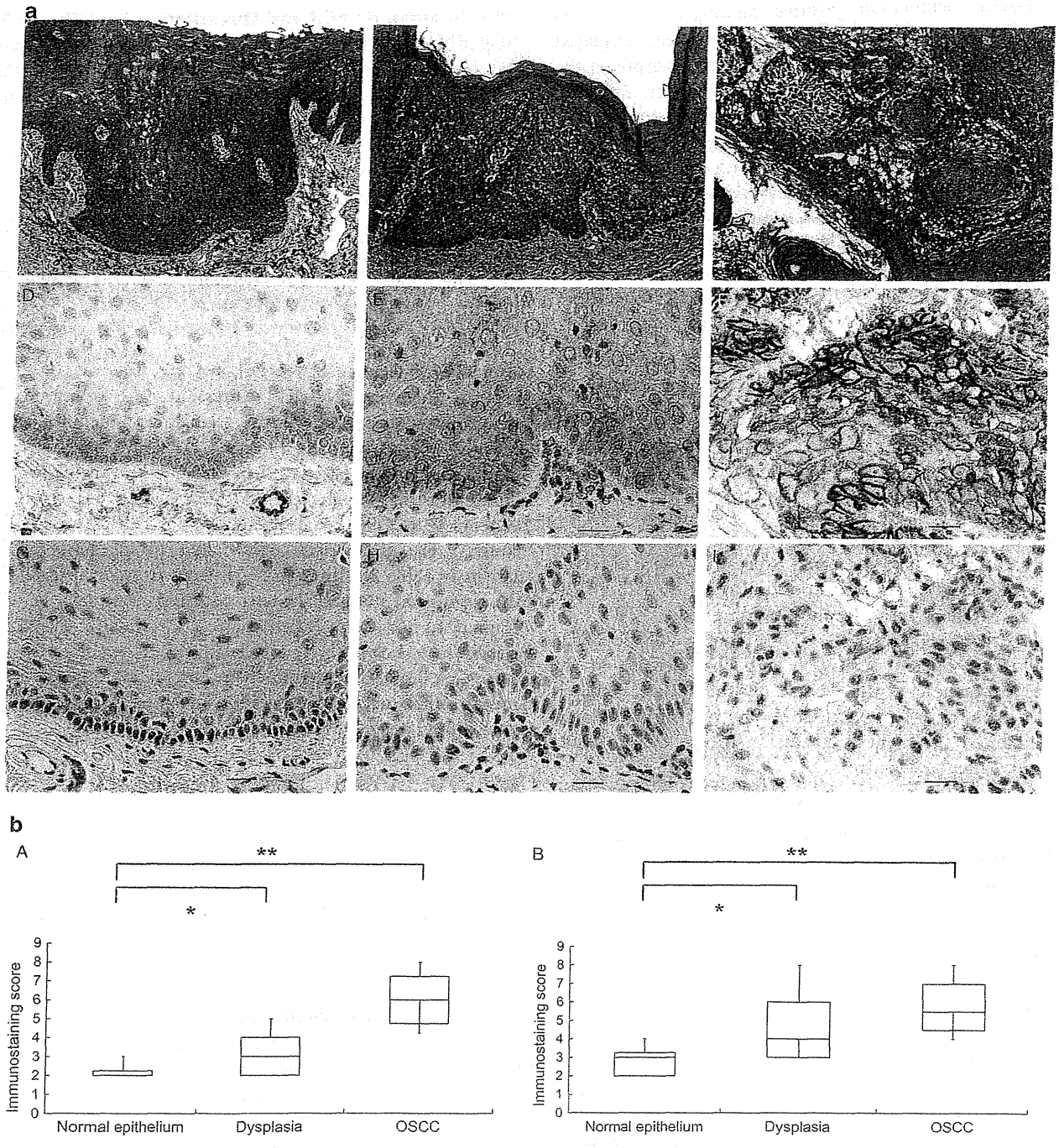

Figure 1 Immunohistochemical staining of Notch1 and its intracytoplasmic domain (NICD) in normal, dysplastic and cancerous tissues of oral mucosa. (**a**) Representative hematoxylin and eosin (H&E) staining photomicrographs in: normal (A), dysplastic (B) and cancerous tissues (C) of oral mucosa. Original magnification, ×100. Scale bar = 100 μm. (D–F) Representative immunohistochemical stainings of Notch1 at each pathological stage in high-power fields. Tissues were immunohistochemically stained using an antibody to Notch1. The membranous immunoreactions (brown) were regarded as positive for Notch1. Original magnification, ×400. Scale bar = 20 μm. (G–I) Representative immunohistochemical stainings of NICD at each clinical stage in high-power fields. Tissues were immunohistochemically stained using an antibody to NICD. The nuclear immunoreactions (brown dots) were regarded as positive for NICD. Original magnification, ×400. Scale bar = 20 μm. (**b**) (A) Graphs of Notch1 immunostaining scores. Immunostaining scores obtained from each pathological group were calculated and statistically analyzed. The mean Notch1 immunostaining score was the highest in the oral squamous cell carcinoma (OSCC) group. The Y axis shows the mean values of the Notch1 immunostaining scores. (B) Graphs of NICD immunostaining scores. Immunostaining scores obtained from each pathological group were calculated and statistically analyzed. The mean NICD immunostaining score was the highest in the OSCC group. The Y axis shows the mean values of the NICD immunostaining scores. NS, no significance; $^{*}P<0.05$; $^{**}P<0.01$, analyzed by one-way analysis of variance (ANOVA) with the Bonferroni/Dunn test.

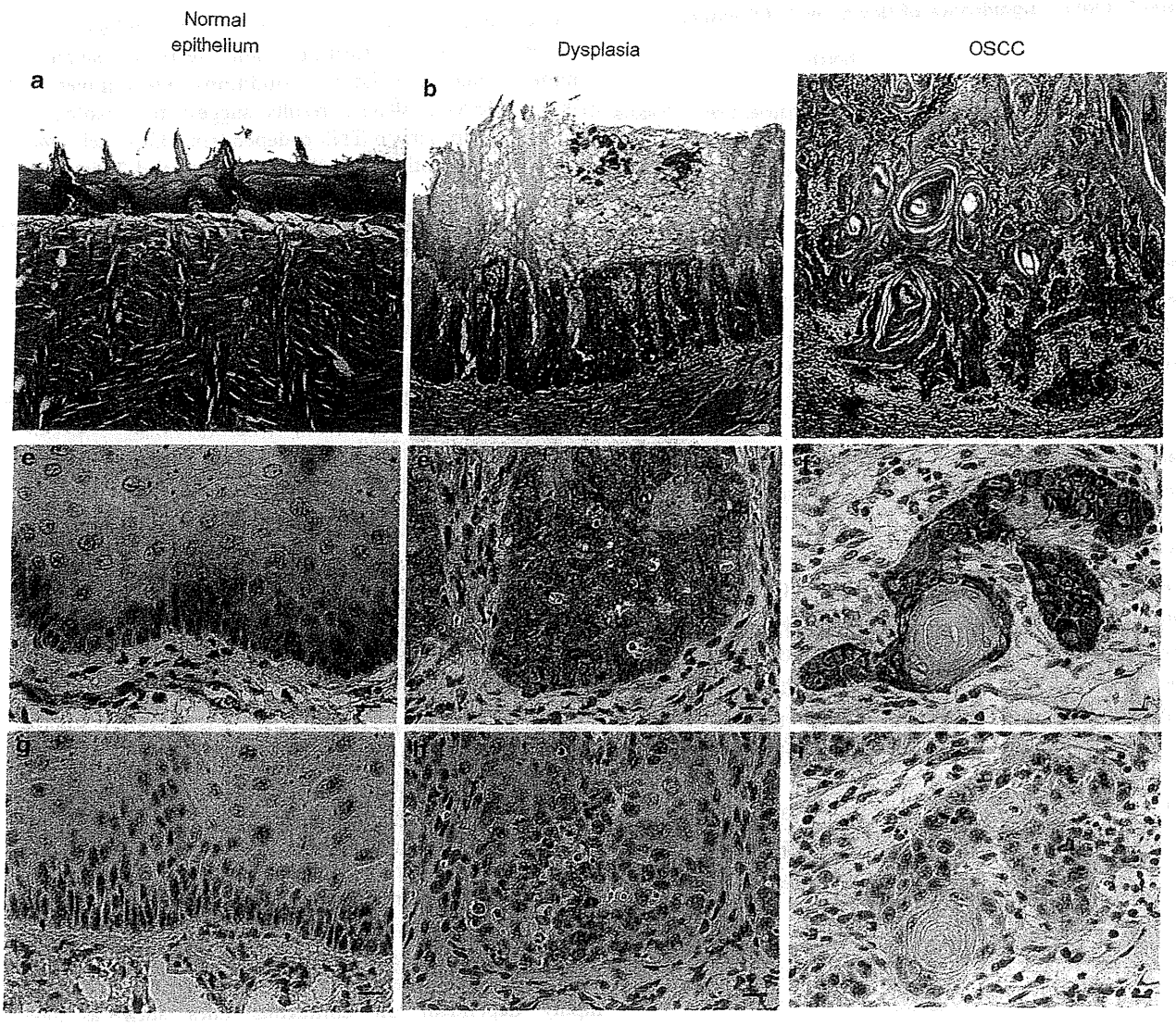

Figure 2 An immunohistochemical analysis of Notch1 in a rat carcinogenesis model. Representative hematoxylin and eosin (H&E) staining photomicrographs of normal (**a**), dysplastic (**b**) and cancerous tissues (**c**) of the tongue obtained from rats used in a rat carcinogenesis model. Original magnification, × 100. Scale bar = 100 μm. (**d–f**) Representative immunohistochemical stainings of Notch1 at each pathological grade in high-power fields. Tissues obtained from rats used in a rat carcinogenesis model were immunohistochemically stained using an antibody to Notch1. The membranous immunoreactions (brown) were regarded as positive for Notch1. Original magnification, × 400. Scale bar = 20 μm. (**g–i**) Representative immunoreactions of Notch1 and intracellular Notch domain (NICD) in high-power fields. Tissues obtained from rats used in a rat carcinogenesis model were immunohistochemically stained using an antibody to NICD. The nuclear immunoreactions (brown dots) were regarded as positive for NICD. In the cancerous tissues, a majority of oral squamous cell carcinoma (OSCC) cells showed strong immunoreactions for NICD. Original magnification, × 400. Scale bar = 20 μm.

TNF α-Dependent OSCC Cell Invasiveness

To determine the significance of Notch1 expression other than proliferation, we further analyzed the expression pattern of Notch1 in the histological samples. In the OSCC specimens, Notch1 was primarily expressed in the cells at the epithelial–stromal interface (Supplementary Figure S3A). Furthermore, NICD was strongly expressed in the cells at the invasive tumor front (Supplementary Figure S3B).

Based on the localizations of Notch1 and NICD observed in the histological analysis, we hypothesized that Notch1 signaling could be involved in the invasiveness of OSCC cells. Therefore, a Matrigel invasion assay was completed to assess whether the Notch1 expression affects the invasiveness of OSCC cells *in vitro*. In this experiment, TNF-α, a well-known accelerator of tumor invasion, was used. TNF-α has been reported to show an increased expression in OSCC specimens[27] and promote S2 cleavage (resulting in NICD

Table 2 Clinical significance of Notch1 in OSCC tissues

Characteristics	Total	Notch1		*P*-value
		Positive, *n* (%)	Negative, *n* (%)	
	54	38 (70.4)	16 (29.6)	
Age (years)				
Median	70.5	70.7	70.1	
Range	51–87	51–86	56–87	
≤65	18	12 (66.7%)	6 (33.3%)	0.673
>65	36	26 (72.2%)	10 (27.8%)	
Gender				
Male	31	21 (67.7%)	10 (32.3%)	0.623
Female	23	17 (73.9%)	6 (26.1%)	
Primary site				
Tongue	13	10 (76.9%)	3 (23.1%)	0.262
Mandible	10	6 (60.0%)	4 (40.0%)	
Maxilla	12	6 (50.0%)	6 (50.0%)	
Oral floor	9	7 (77.8%)	2 (22.2%)	
Buccal mucosa	10	9 (90.0%)	1 (10.0%)	
T-stage				
T1, T2	19	12 (63.2%)	7 (36.8%)	0.019*
T3	18	17 (94.4%)	1 (5.6%)	
T4	17	9 (52.9%)	8 (47.1%)	
Nodal stage				
≤1	31	21 (67.7%)	10 (32.3%)	0.077
>2a	19	17 (89.5%)	2 (10.5%)	
Clinical stage				
II	4	1 (25.0%)	3 (75.0%)	0.005**
III	19	18 (94.7%)	1 (5.3%)	
IV	31	19 (61.3%)	12 (38.7%)	
Differentiation				
Well	40	28 (70.0%)	12 (30.0%)	0.920
Moderate	14	10 (71.4%)	4 (28.6%)	

The χ^2-test was used to examine the relationship between the Notch1 expression and the clinicopathologic factors. *$P<0.05$; **$P<0.01$.
Fisher's exact test was used when one or more cells had expected values <5.

observed in the Stat3, MAPK or Akt pathways or in the expressions of matrix metalloproteinase (MMP)-2 or -9 (data not shown). However, mRNAs of Slug and Twist, critical transcriptional factors that control cell invasion,[31] were affected by TNF-α treatment and decreased significantly under Notch1 knockdown conditions (see Supplementary Figures S5A–C). These results suggest that Notch1 may contribute in part to TNF-α-dependent OSCC cell invasion via the transcriptional regulation of Slug and Twist.

GSI Inhibits the Proliferation, Migration and Invasion of OSCC Cells

To test the possible application of GSI in the treatment of OSCC, SAS cells were treated with GSI or a control vehicle (DMSO) and cell proliferation, migration and invasiveness were assessed. As shown in Figure 7a, GSI significantly inhibited cell proliferation in a dose-dependent manner ($P<0.05$). Using western blotting, decreased expressions of NICD, Hes1, p-H3 and p-Akt were confirmed. Furthermore, the number of invaded cells enhanced by TNF-α was significantly decreased under the GSI treatment conditions (Figure 7c; *P*-value <0.01). These results suggest that GSI has a potential for clinical use in OSCC treatment.

DISCUSSION

Notch1 and its signaling have been examined in various types of cancer. Although the oncogenic role of Notch signaling in T-ALL is well established,[32] a common theme for the role of Notch signaling in tumorigenesis remains elusive. In many types of solid tumor, including cancers of the lung,[11] breast,[16] pancreas[13] and prostate.[14] Notch1 signaling therefore seems to have a crucial role. Notch1 signaling also appears to have tumor suppressor roles in murine keratinocytes,[20] human pancreatic[19] and hepatocellular carcinomas[18] and small-cell lung cancer.[33] Taken together, these observations indicate that aberrant activation of the Notch1 pathway has various roles in solid tumors. Moreover, the cellular reactions and outcomes of the overexpression of Notch1 activity are highly dependent on contextual cues such as interactions with the tumor microenvironment and crosstalk with other signaling pathways. Our present report provides an extensive evaluation of Notch1 expression in human OSCC tissues and the effects of Notch1 expression in OSCC cell lines.

Strong Notch1 expression was seen in the cell membrane of oral cancer cells in our present study, whereas a weak and limited expression was observed in the basal layer in normal tissues. In previous studies, the overexpression of Notch1 and its ligands has been observed in OSCC specimens.[34,35] However, a recent study demonstrated opposite results to this study. The study of Sakamoto *et al*[24] showed similar Notch1 expression to that observed in our study in normal tissues, whereas their results for dysplastic and cancerous tissues were different, and Notch1 was downregulated in the neoplastic lesions.Although the antibodies against Notch1 and staining method used in our study were different from those used by Sakamoto *et al*,[24] our immunohistochemical staining results showed clear and specific membranous

positively immunostained for Notch1. To strengthen our immunohistochemical study furthermore, we reinvestigated Notch1 expression in a rat carcinogenesis model useful for monitoring cancer-progression-related molecules. In the sequential analysis model of tongue carcinogenesis, the Notch1 expression exhibited the same tendency as that observed in the human tissue specimens. These results encouraged us to conclude that Notch1 overly accumulates or overexpresses and may have certain roles in the late stage of carcinogenesis and OSCC.

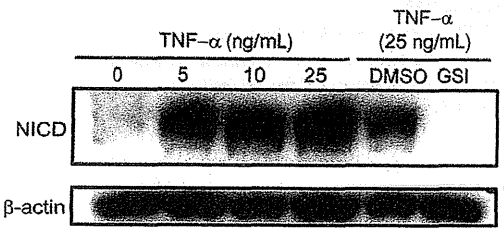

Figure 5 Effect of tumor necrosis factor (TNF)-α on Notch1 and intracellular Notch domain (NICD) cleavage in SAS cells. SAS cells were incubated with various concentrations of TNF-α alone or with dimethyl sulfoxide (DMSO) and γ-secretase inhibitor (GSI) for 24 h, and then examined for NICD cleavage by western blot.

In our clinicopathological analysis, a high level of Notch1 expression was found to be correlated with both T-stage and clinical stage in patients with OSCC. Although a statistical correlation was not observed, an increasing percentage of patients with Notch1-positive cancers showed advanced Nodal status. These results indicate that Notch1 has a potential role in OSCC progression. In addition, similar to our present study, two reports have described the clinical significance of Notch1 expression in HNSCCs, including OSCC.[36,37] Therefore, we concluded that Notch1 may have an important role in OSCC progression.

Based on the histological findings observed in the human and rat OSCC samples, we hypothesized that Notch1 regulates the proliferation and invasiveness of OSCC cells. This was confirmed *in vitro*. First, we examined the expressions of Notch1, its related molecules and NICD, which indicates the activation of Notch1 signaling, in a panel of OSCC cell lines. Second, we investigated whether the Notch1 expression affects the proliferation of cultured OSCC cells using *Notch1*-specific siRNA and a WST assay, as the importance of the Notch1 expression for cell proliferation is well known and has been previously examined.[38–40] Most of OSCC cell lines expressed Notch1 signaling molecules and NICD, and Notch1 knockdown significantly inhibited cell proliferation

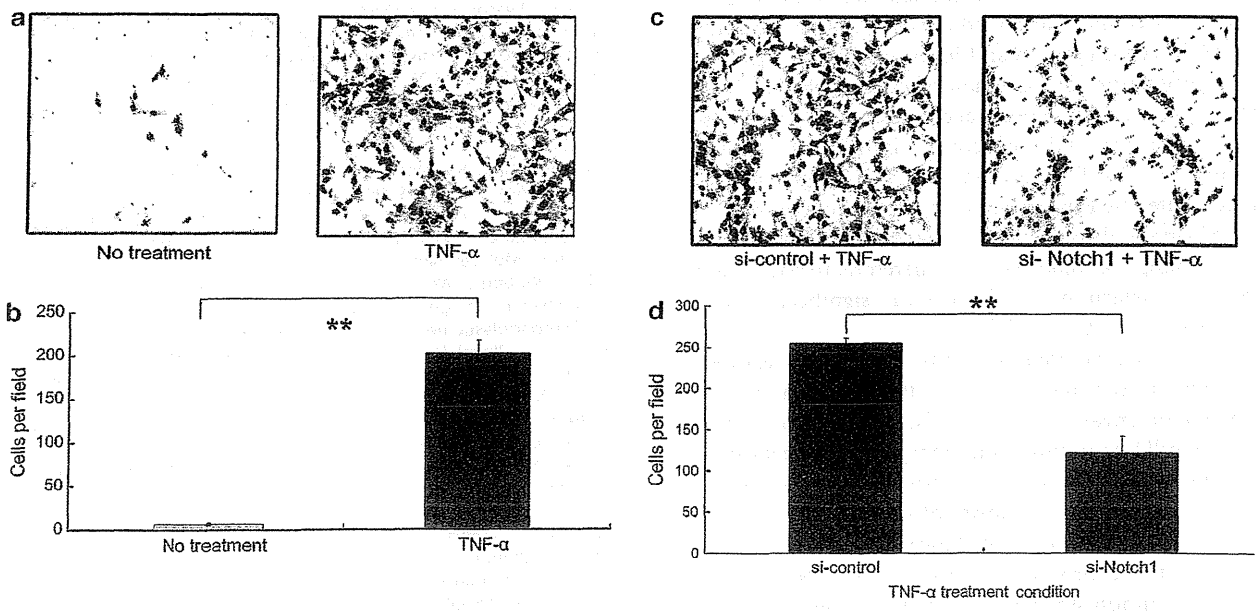

Figure 6 Effects of *Notch1* small interfering RNA (siRNA) on SAS cell invasion. (**a**, **b**) The effects of tumor necrosis factor (TNF-α) treatment on SAS cell invasion. SAS cells were incubated with either control or *Notch1*-specific siRNA for 24 h in the presence of TNF-α. The numbers of invaded cells obtained from three independent experiments were counted and statistically analyzed. The photos are representative fields of invasive cells on the membranes. TNF-α markedly activated the invasive properties of the cells. Original magnification, × 100. The bar graphs represent the average numbers of cells on the underside of the membranes. The Y axis shows the numbers of cells invading the underside of the membranes. Mean ± s.d. of three independent experiments. $^{**}P<0.01$, analyzed by Student's *t*-test. (**c**, **d**) The effects of *Notch1* siRNA on TNF-α-dependent SAS cell invasion. The photos are representative fields of invasive cells on the membranes. TNF-α-dependent activation of tumor invasion was significantly inhibited under *Notch1* knockdown conditions. Original magnification, × 100. The bar graphs represent the average numbers of cells on the underside of the membranes. The Y axis shows the numbers of cells invading the underside of the membranes. Mean ± s.d. of three independent experiments. $^{**}P<0.01$, analyzed by Student's *t*-test.

expression affects the proliferation of cultured OSCC cell lines via Akt signaling. In OSCC, Akt signaling has an important role in its progression,[41,42] and inhibition of Akt signaling suppresses malignant phenotype.[43]

Recently, growing evidence has indicated a relationship between Notch signaling and tumor cell invasion.[44,45] Our present data demonstrated that the Notch1 expression influences the TNF-α-dependent invasiveness of OSCC cells via the transcriptional regulation of Slug and Twist, important regulators of cell invasion.[31] Several reports have described the significance of Notch signaling for the invasiveness of squamous cell carcinomas, including those of the oral cavity. In these reports, MMPs, the nuclear factor-κB pathway and micro-RNAs were reported to be associated with increases in invasive phenotypes.[46,47] Our data support these previous findings and we conclude that Notch1 has a role in a certain type of OSCC invasion. However, we need further investigation to determine what mechanisms underlie the invasiveness of OSCC cells because Notch signaling shows cross-talk with many other pathways and regulates the properties of these pathways based on complicated mechanisms.

GSI prevents the activation of Notch signaling, and several Notch inhibitors have been tested for antitumor effects.[48] Our present data clearly demonstrated that treatment of OSCC cells with GSI effectively reduces the NICD/Hes1 protein expression and prevents growth in OSCC cell lines, similar to that observed in Notch1 knockdown conditions. In our study, GSI treatment inhibited not only cell proliferation but also OSCC cell migration and invasion. Similar effects of GSI on the migration and invasion of cancer cells has been reported in pancreatic cancer and melanoma.[49,50] These findings suggest that GSI effectively inhibits the Notch pathway in OSCC cell lines and that the progression of OSCC is regulated by this signaling system. Recently, another effect of GSI on the drug resistance phenotype of cancer cells in Notch signaling was reported.[51,52] Therefore, further study is required to determine the biological significance and antitumor effects of GSI in OSCC.

In conclusion, we demonstrated that the Notch1 expression is involved in the maintenance of the proliferation and TNF-α-dependent invasiveness of OSCC cells. Although the use of a single cell line in functional analysis is a limitation of this study, the expressions of NICD, which indicates activation of Notch signaling, in majority of OSCC cell lines and OSCC specimens were confirmed. Moreover, positive correlation between the expressions of Notch1 and NICD was observed in immunohistochemical analysis. Therefore, the activation of Notch signaling may occur in the other cell lines and clinical OSCC. Indeed, one report has demonstrated the tumor suppressor functions of Notch signaling based on the findings of loss-of-function mutations of Notch1 in HNSCC.[53] However, in that report, this type of mutation was detected in a certain subset of patients having HNSCC. Therefore, considering the previous studies of HNSCCs,[34,46] including OSCC that indicate the oncogenic functions of Notch1 and the context dependency of Notch signaling, certain types of OSCC cells may require Notch1 expression for progression. Moreover, GSI, a pharmacological agent known to effectively block Notch1 activation, was found to inhibit the proliferation, migration and invasiveness of OSCC cells, which suggests the potential for using GSI in OSCC treatment.

Supplementary Information accompanies the paper on the Laboratory Investigation website (http://www.laboratoryinvestigation.org)

ACKNOWLEDGEMENTS

We thank Mr Shinji Kudo, Mrs Motoko Kagayama, Mrs Takako Maeda and Mrs Hiroko Kouzuma for their skillful technical assistance. This study was partly supported by a Grant-in-Aid for Scientific Research (C; No. 21590440) from Ministry of Education, Culture, Sports, Science and Technology of Japan.

DISCLOSURE/CONFLICT OF INTEREST

The authors declare no conflict of interest.

1. Siegel R, Naishadham D, Jemal A. Cancer statistics, 2012. CA Cancer J Clin 2012;62:10–29.
2. Gupta S, Kong W, Peng Y, *et al.* Temporal trends in the incidence and survival of cancers of the upper aerodigestive tract in Ontario and the United States. Int J Cancer 2009;125:2159–2165.
3. Napier SS, Speight PM. Natural history of potentially malignant oral lesions and conditions: an overview of the literature. J Oral Pathol Med 2008;37:1–10.
4. Barnes L, Eveson JW, Reichart P, *et al.* Pathology and Genetics of Head and Neck Tumours. IARC Press: Lyon, 2005, pp 177–180.
5. Warnakulasuriya S. Histological grading of oral epithelial dysplasia: revisited. J Pathol 2001;194:294–297.
6. Artavanis-Tsakonas S, Rand MD, Lake RJ. Notch signaling: cell fate control and signal integration in development. Science 1999;284: 770–776.
7. Gray GE, Mann RS, Mitsiadis E, *et al.* Human ligands of the Notch receptor. Am J Pathol 1999;154:785–794.
8. Wu L, Sun T, Kobayashi K, *et al.* Identification of a family of mastermind-like transcriptional coactivators for mammalian notch receptors. Mol Cell Biol 2002;22:7688–7700.
9. Ellisen LW, Bird J, West DC, *et al.* TAN-1, the human homolog of the *Drosophila* notch gene, is broken by chromosomal translocations in T lymphoblastic neoplasms. Cell 1991;66:649–661.
10. Puente XS, Pinyol M, Quesada V, *et al.* Whole-genome sequencing identifies recurrent mutations in chronic lymphocytic leukaemia. Nature 2011;475:101–105.
11. Westhoff B, Colaluca IN, D'Ario G, *et al.* Alterations of the Notch pathway in lung cancer. Proc Natl Acad Sci USA 2009;106:22293–22298.
12. Weijzen S, Rizzo P, Braid M, *et al.* Activation of Notch-1 signaling maintains the neoplastic phenotype in human Ras-transformed cells. Nat Med 2002;8:979–986.
13. Miyamoto Y, Maitra A, Ghosh B, *et al.* Notch mediates TGF alpha-induced changes in epithelial differentiation during pancreatic tumorigenesis. Cancer Cell 2003;3:565–576.
14. Zayzafoon M, Abdulkadir SA, McDonald JM. Notch signaling and ERK activation are important for the osteomimetic properties of prostate cancer bone metastatic cell lines. J Biol Chem 2004;279:3662–3670.
15. Santagata S, Demichelis F, Riva A, *et al.* JAGGED1 expression is associated with prostate cancer metastasis and recurrence. Cancer Res 2004;64:6854–6857.
16. Reedijk M, Odorcic S, Chang L, *et al.* High-level coexpression of JAG1 and NOTCH1 is observed in human breast cancer and is associated with poor overall survival. Cancer Res 2005;65:8530–8537.
17. Klinakis A, Lobry C, Abdel-Wahab O, *et al.* A novel tumour-suppressor function for the Notch pathway in myeloid leukaemia. Nature 2011;473:230–233.

SpringerPlus
a SpringerOpen Journal

RESEARCH Open Access

(–)-Epigallocatechin-3-gallate suppresses hepatic preneoplastic lesions developed in a novel rat model of non-alcoholic steatohepatitis

Takafumi Sumi[1], Yohei Shirakami[1], Masahito Shimizu[1,3*], Takahiro Kochi[1], Tomohiko Ohno[1], Masaya Kubota[1], Makoto Shiraki[1], Hisashi Tsurumi[1], Takuji Tanaka[2] and Hisataka Moriwaki[1]

Abstract

Purpose: Non-alcoholic fatty liver disease (NAFLD) ranges from simple steatosis to non-alcoholic steatohepatitis (NASH). NASH, which is accompanied by increased oxidative stress and inflammation in the liver, is associated with hepatic carcinogenesis. Green tea catechins (GTCs) possess anti-oxidant, anti-inflammatory, and cancer-preventive properties. In this study, we investigated whether (–)-epigallocatechin-3-gallate (EGCG), a major component of GTCs, inhibits NAFLD/NASH-related liver tumorigenesis.

Methods: Male 8-week-old Sprague–Dawley (SD) rats were administered a single intraperitoneal injection of a hepatic carcinogen diethylnitrosamine (DEN, 30 mg/kg body weight) and then fed a high-fat diet (HFD) for 7 weeks. The rats were also provided tap water containing 0.01% or 0.1% EGCG during the experiment.

Results: At sacrifice, the livers of SD rats treated with DEN and HFD exhibited marked development of glutathione *S*-transferase placental form (GST-P)-positive foci, a hepatic preneoplastic lesion, and this was associated with hepatic steatosis, oxidative stress and inflammation, and hepatocyte proliferation. EGCG administration, however, inhibited the development of GST-P-positive foci by decreasing hepatic triglyceride content, reducing hepatic fibrosis, lowering oxidative stress, attenuating inflammation, and inhibiting excessive hepatocyte proliferation in DEN- and HFD-treated SD rats. These findings suggest that the experimental model of SD rats treated with HFD and DEN, in which histopathological and pathophysiological characteristics of NASH and the development of hepatic premalignant lesions were observed, might facilitate the evaluation of liver tumorigenesis associated with NAFLD/NASH.

Conclusions: Administering EGCG, a GTC, might serve as an effective chemoprevention modality for NAFLD/NASH-related liver tumorigenesis.

Keywords: Non-alcoholic steatohepatitis; Liver tumorigenesis; Oxidative stress; Inflammation; EGCG

Background

Non-alcoholic fatty liver disease (NAFLD), which is considered a hepatic manifestation of the metabolic syndrome, is currently one of the most common chronic liver diseases worldwide. NAFLD is classified into simple steatosis and non-alcoholic steatohepatitis (NASH), the latter being a severe condition of inflamed fatty liver that can, in time, lead to hepatic fibrosis, cirrhosis, hepatocellular carcinoma (HCC) development, and result in increased mortality (Chiang et al., 2011; Cusi, 2012; Siegel and Zhu, 2009). Steatohepatitis has been indicated by epidemiological studies to be a significant risk factor for developing HCC, at an annual HCC incidence of 2%–3% in patients with NASH (Adams et al., 2005; Ascha et al., 2010). In 1998, Day and James proposed a "two-hit theory" to explain NAFLD/NASH pathogenesis: the first hit, hepatic steatosis, increases the sensitivity of the liver to proinflammatory insults, while the second hit involves oxidative stress (Day and James, 1998). Oxidative

* Correspondence: shimim-gif@umin.ac.jp
[1]Department of Internal Medicine, Gifu University Graduate School of Medicine, Gifu, Japan
[3]Department of Internal Medicine/Gastroenterology, Gifu University Graduate School of Medicine, 1-1 Yanagido, Gifu 501-1194, Japan
Full list of author information is available at the end of the article

stress, which is associated with HCC development (Suzuki et al., 2013), is substantially higher in NASH patients than in NAFLD patients and normal control subjects (Sanyal et al., 2001). Moreover, tumor necrosis factor (TNF)-α and interleukin (IL)-6, both of which are major proinflammatory cytokines, play a critical role in obesity-related steatohepatitis and subsequent liver tumorigenesis (Park et al., 2010).

Several animal models that mimic the pathophysiological mechanisms associated with NAFLD/NASH-related liver carcinogenesis have been developed recently (Hebbard and George, 2011; Schattenberg and Galle, 2010; Kochi et al., 2013). For instance, *db/db* mice, which exhibit obesity, diabetes, dyslipidemia, and severe steatosis, are susceptible to liver tumorigenesis induced by a hepatic carcinogen diethylnitrosamine (DEN), and thus are regarded as useful animal models for investigating pathobiology of NAFLD/NASH-related liver carcinogenesis and for screening the chemopreventive effects of various compounds either synthetic or natural on NAFLD/NASH-related liver carcinogenesis (Iwasa et al., 2010; Shimizu et al. 2011a, 2011b, 2011c). Recently, Wang et al. (Wang et al. 2009) reported that NASH induced by a high-fat diet (HFD) promoted DEN-initiated early hepatocarcinogenesis in Sprague–Dawley (SD) rats and that this was associated with increased oxidative stress and inflammation. This animal model is also useful for investigating the efficacy of certain types of synthetic compounds and/or phytochemicals in preventing NASH-promoted liver carcinogenesis (Wang et al., 2010).

The prevalence of NAFLD/NASH has risen recently in parallel with the dramatic increase in obesity and its related metabolic abnormalities, especially diabetes mellitus (Chiang et al., 2011; Cusi, 2012; Siegel and Zhu, 2009), indicating an urgent requirement for developing an effective strategy to treat NAFLD/NASH and, consequently, to prevent NAFLD/NASH-related liver carcinogenesis. A recent randomized trial (Sanyal et al., 2010) has shown that treatment with vitamin E, an antioxidant, reduces steatosis and lobular inflammation in the liver of NASH patients. Reducing oxidative stress and inhibiting the inflammation induced by obesity and steatosis are also effective in preventing obesity- and diabetes-related hepatotumorigenesis (Shimizu et al. 2013, 2012). These reports suggest that targeting oxidative stress and chronic inflammation is an optimal strategy for preventing NAFLD/NASH-related liver carcinogenesis.

Green tea catechins (GTCs) might be one of the most promising candidate compounds for preventing NAFLD/NASH-related liver carcinogenesis because they are considered to protect against metabolic disorders such as NAFLD (Masterjohn and Bruno, 2012; Thielecke and Boschmann, 2009) and also display cancer chemopreventive properties in various tissues, including the liver (Shimizu et al. 2011b; Kochi et al., 2013; Yang et al., 2009). In this study, we developed a novel rat model of NAFLD/NASH-related carcinogenesis and investigated the potential capacity of (−)-epigallocatechin-3-gallate (EGCG), a major component of GTCs, to inhibit the occurrence of HFD- and DEN-induced glutathione *S*-transferase placental form (GST-P)-positive foci, an indicator of preneoplastic HCC lesions in rats (Tsuda et al., 2003; Ando et al., 2007).

Results

General observations

At the end of the experimental period, the rats in the 3 groups exhibited no significant differences with respect to the mean body, liver, and kidney weights (Table 1). Histopathological examination revealed that administering EGCG produced no detectable toxic effects on critical organs including the liver, kidney, and spleen (data not shown).

Effects of EGCG on hepatic steatosis and serum ALT levels in rats

At sacrifice, macrovesicular steatosis with ballooned hepatocytes, Mallory-Denk bodies, and foci of inflammatory cells, which are a recognized feature of NASH (Kleiner et al., 2005), were observed in the livers of rats in all groups, indicating that the histopathological characteristics that develop in this animal model reproduce those of NASH. However, these pathological effects were alleviated by the administration of 0.01% and 0.1% EGCG (Figure 1a and 1b). In particular the total NAFLD activity score (NAS) consisting of the steatosis, inflammation, and ballooning scores, was significantly lower in 0.1% EGCG-treated rats than in EGCG-untreated control rats (Figure 1c, $P < 0.05$). Similar results were obtained following measurement of intrahepatic lipid content: the levels of liver triglycerides in

Table 1 Body and organ weights of the experimental rats

Group No.	EGCG	No. of rats	Body weight (g)	Relative organ weight (g/100 g body weight)	
				Liver	Kidneys
1	-	7	512.7 ± 37.8[a]	3.8 ± 0.5	0.6 ± 0.4
2	0.01%	6	495.5 ± 29.0	3.9 ± 0.6	0.7 ± 0.3
3	0.1%	6	501.6 ± 44.3	3.5 ± 0.2	0.6 ± 0.3

[a]Mean ± SD.

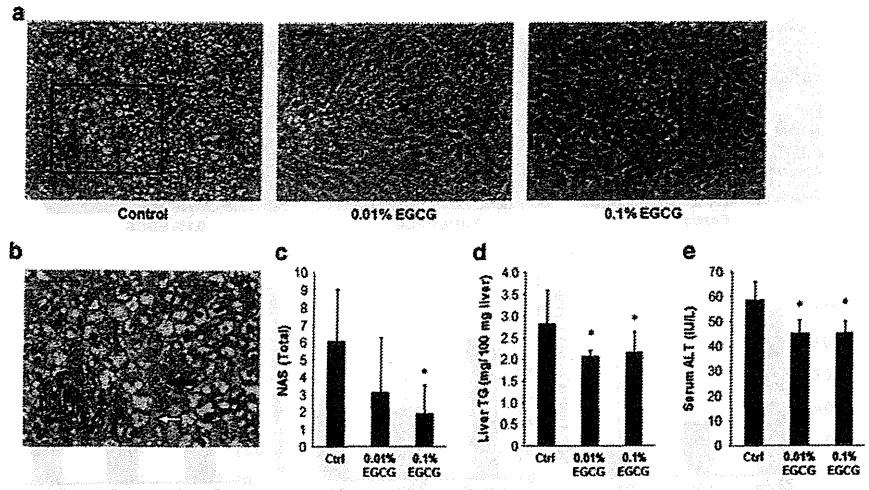

Figure 1 Hepatic histopathology, intrahepatic levels of triglycerides, and serum levels of ALT. (a) and **(b)** H&E staining of liver sections from the experimental rats. **(a)** Representative photomicrographs of liver sections of rats treated DEN/HFD with or without EGCG. Bars, 100 μm. **(b)** An enlarged photo of the liver section from a rat treated DEN/HFD without EGCG (an enclosed area with square in Figure 1a). Note ballooned hepatocytes (indicated by the white arrow), Mallory-Denk bodies (indicated by the black arrow), and focus of inflammatory cells (circled by dotted line). Bars, 50 μm. **(c)** The NAS was determined from histopathological analysis. **(d)** Hepatic lipids were extracted from frozen liver samples of rats in the 3 groups, and the triglyceride (TG) levels were measured. **(e)** Blood samples were collected at sacrifice and the serum levels of alanine aminotransferase (ALT) were determined. The values are expressed as mean ± SD. *$P < 0.05$. Ctrl, control group.

the DEN- and HFD-treated SD rats were significantly decreased when they received 0.01% and 0.1% EGCG instead of water (Figure 1d, $P < 0.05$). The serum alanine aminotransferase (ALT) levels were also significantly decreased with EGCG treatment at both concentrations relative to the levels in the water-treated group (Figure 1e, $P < 0.05$), indicating that EGCG protected against hepatic steatosis and subsequent hepatocyte injury induced by DEN and HFD.

Effects of EGCG on liver fibrosis in rats

Examination of Azan-stained liver sections revealed that DEN- and HFD-treated SD rats developed perisinusoidal fibrosis, but that EGCG administration reduced liver fibrosis in the animals (Figure 2a). The liver fibrosis score was also significantly decreased by EGCG administration (Figure 2b). Furthermore, EGCG treatment significantly lowered (relative to control) the hepatic levels of TIMP-1 and TIMP-2 mRNA in the DEN- and HFD-treated SD rats (Figure 2c, $P < 0.05$).

Effects of EGCG on the development of hepatic preneoplastic lesions in rats

At the end of the experiment, GST-P-positive foci were detected in the livers of the rats, all of which had received DEN/HFD (Figure 3a). However, compared with rats in the control group that were not treated with EGCG, rats treated with EGCG showed a significant reduction in the number of GST-P-positive foci: 86% and 87% reduction relative to control following treatment with 0.01% and 0.1% EGCG, respectively (Figure 3b, $P < 0.01$).

Effects of EGCG on oxidative stress in rats

Oxidative stress plays a critical role in the NAFLD-to-NASH progression and HCC development (Chiang et al., 2011; Cusi, 2012; Siegel and Zhu, 2009). Therefore, we examined the levels of oxidative stress and antioxidant biomarkers in the experimental rats. Rats administrated with 0.1% EGCG had significantly reduced levels of urinary 8-OHdG, a marker of DNA damage induced by oxidative stress, compared with EGCG-untreated control rats (Figure 4a, $P < 0.01$). The serum d-ROM level, which reflects serum hydroperoxide levels, was also decreased relative to control in rats treated with 0.01% and 0.1% EGCG (Figure 4b, $P < 0.01$). Moreover, the antioxidant enzyme (catalase and GPx-1) levels were significantly increased in the livers of rats that received EGCG treatment (Figure 4c, $P < 0.05$). These results indicate that drinking EGCG attenuated both systemic and hepatic oxidative stress in our rat model of NAFLD/NASH-related liver tumorigenesis.

Effects of EGCG on hepatic expression of TNF-α, IL-6, and IL-1β mRNA in rats

Chronic inflammation is implicated in the progression of NASH and subsequent liver carcinogenesis (Chiang et al., 2011; Cusi, 2012; Siegel and Zhu, 2009; Park et al., 2010). Therefore, the mRNA expression levels of 3 inflammatory

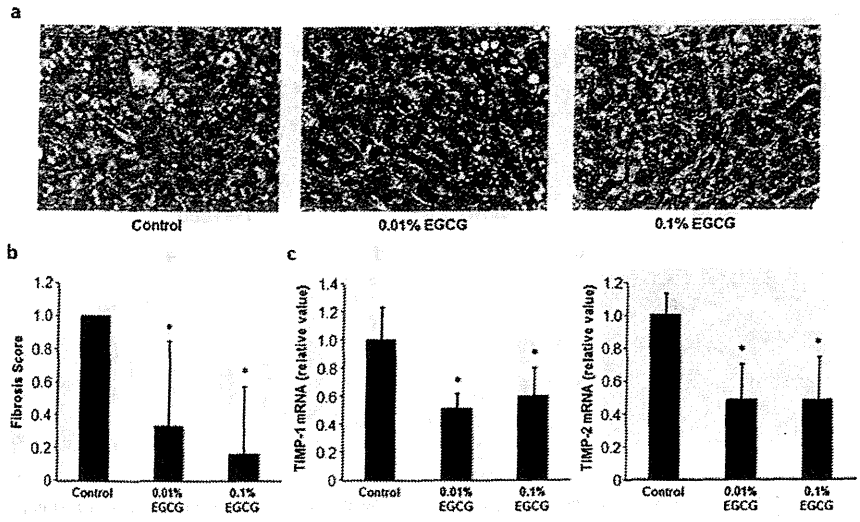

Figure 2 Liver fibrosis and hepatic expression levels of TIMP-1 and TIMP-2 mRNA. (a) Representative photomicrographs of Azan staining of liver tissues to show fibrosis. Bars, 50 μm. Note reduction of liver fibrosis (blue) by the treatment with EGCG. **(b)** Liver fibrosis evaluation was based on the NAS system. **(c)** After total RNA was isolated from the livers of the rats, the levels of TIMP-1 and TIMP-2 mRNA were measured using specific primers and quantitative real-time RT-PCR. The values are expressed as mean ± SD. * $P < 0.05$.

mediators, TNF-α, IL-6, and IL-1β, were measured in the livers of DEN- and HFD-treated SD rats. As shown in Figure 5, quantitative real-time RT-PCR analysis revealed that rats that received 0.1% EGCG exhibited significantly lower hepatic levels of TNF-α ($P < 0.05$), IL-6 ($P < 0.01$), and IL-1β ($P < 0.05$) mRNA than control rats that received only water, and the hepatic levels of IL-6 mRNA were also decreased by the administration of a low dose (0.01%) of EGCG ($P < 0.01$).

Effects of EGCG on hepatocyte proliferation and hepatic expression of cyclin D1 mRNA in rats

The PCNA-labeling index of non-lesional hepatocytes in DEN- and HFD-treated SD rats was determined based on the findings of immunohistochemical examination of sections (Figure 6a). The mean PCNA-labeling indices measured for rats administered 0.01% and 0.1% EGCG were significantly lower than that for EGCG-untreated control rats (Figure 6b, $P < 0.01$). Furthermore, the levels

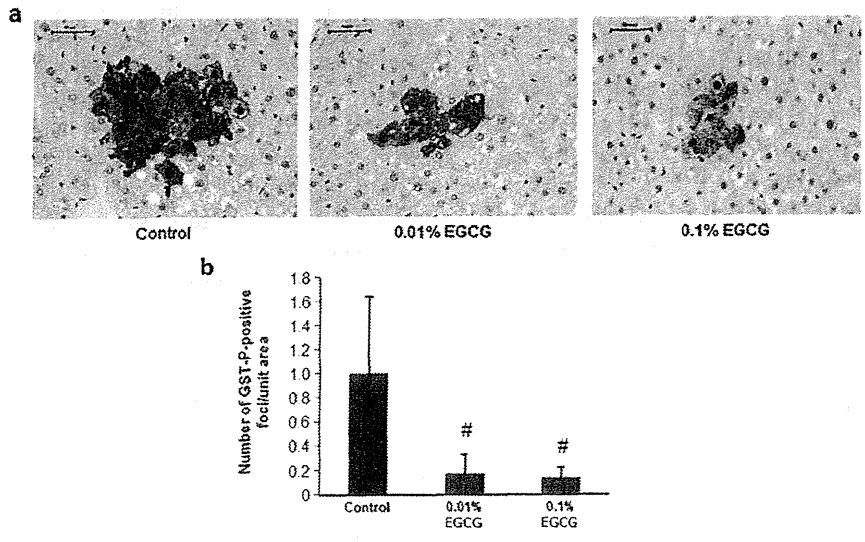

Figure 3 The development of GST-P-positive foci in the livers. (a) Representative photomicrographs of GST-P-positive foci. Note a large GST-P focus in a rat treated with DEN/HFD. Bars, 50 μm. **(b)** The average numbers of GST-P-positive foci formed in the livers of the rats in the 3 groups. The values are expressed as mean ± SD. # $P < 0.01$.

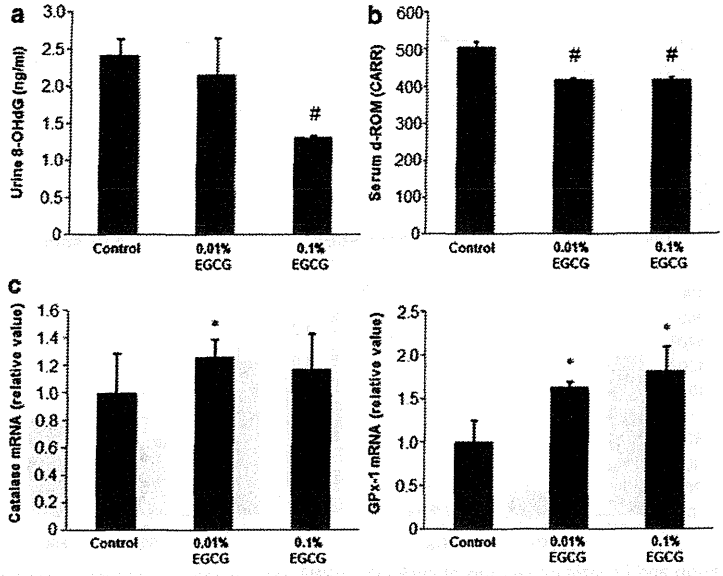

Figure 4 Urinary 8-OHdG and serum d-ROM levels and on the hepatic catalase and GPx-1 mRNA levels. (a) The urinary 8-OHdG levels were measured using ELISA. **(b)** Hydroperoxide levels in the serum were determined using the d-ROM test. **(c)** Levels of catalase and GPx-1 mRNA in the livers of the experimental rats were measured using specific primers and quantitative real-time RT-PCR. The values are expressed as mean ± SD. #P <0.01, *P <0.05.

of cyclin D1 mRNA in liver were also markedly decreased in EGCG-treated rats relative to that in control rats (Figure 6c, $P < 0.05$), indicating that EGCG significantly inhibited hepatocyte proliferation in DEN- and HFD-treated SD rats.

Discussion

An increase in the prevalence of NAFLD/NASH, which can progress to HCC, is a major healthcare problem worldwide (Chiang et al., 2011; Cusi, 2012; Siegel and Zhu, 2009). Therefore, developing an effective strategy for preventing NAFLD/NASH-related liver tumorigenesis is critical for improving the prognosis of patients with these diseases. The results of this study clearly indicate that EGCG, a GTC, effectively prevents the development of hepatic preneoplastic lesions, which manifest as GST-P-positive foci, in our rat model of NAFLD/NASH-related liver tumorigenesis. The rodent model used in this study, which was modified from a model described previously (Wang et al., 2009), reflects the pathological alterations implicated in NAFLD/NASH and NAFLD/NASH-related liver tumorigenesis, including the induction of oxidative stress and chronic inflammation (Chiang et al., 2011; Cusi, 2012; Siegel and Zhu, 2009; Park et al., 2010). Therefore, we consider the present model to be an appropriate and a useful animal model for analyzing the mechanisms of NAFLD/NASH-related liver tumorigenesis and for evaluating the efficacy of specific chemopreventive agents that can suppress such tumorigenesis.

Among the numerous pathophysiological conditions associated with NAFLD/NASH, oxidative stress is regarded as one of the key mechanisms for the development of

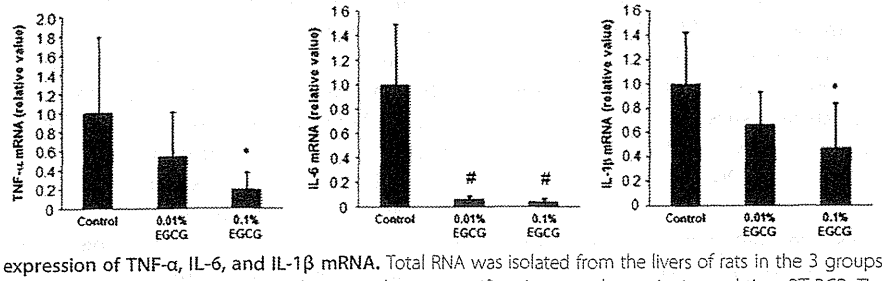

Figure 5 Hepatic expression of TNF-α, IL-6, and IL-1β mRNA. Total RNA was isolated from the livers of rats in the 3 groups and the expression levels of TNF-α, IL-6, and IL-1β mRNA were determined using specific primers and quantitative real-time RT-PCR. The values are expressed as mean ± SD. # P <0.01, *P <0.05.

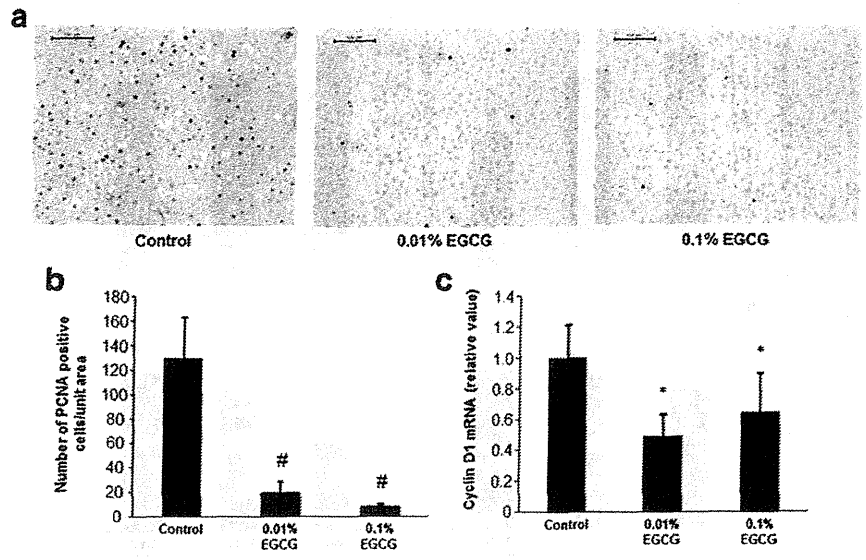

Figure 6 Hepatocyte proliferation and hepatic expression of cyclin D1 mRNA. (a) Immunohistochemical labeling for PCNA in the livers of the experimental rats. Bars, 100 μm. **(b)** The PCNA-labeling index in non-lesional hepatocytes was determined by counting the hepatocytes with PCNA-positive nuclei to calculate their percentage in the hepatocyte population. **(c)** The cyclin D1 mRNA levels in the liver of the experimental rats were determined using specific primers and quantitative real-time RT-PCR. The values are expressed as mean ± SD. # P <0.01, *P <0.05.

HCC. In the progression of NAFLD to NASH, an increase in oxidative stress, which is defined as the overproduction of reactive oxygen species combined with inadequate anti-oxidative defense mechanisms, produces DNA damage and gene mutations associated with liver carcinogenesis (Chiang et al., 2011; Cusi, 2012; Siegel and Zhu, 2009; Park et al., 2010). Conversely, treatment with antioxidants such as vitamin E can reduce hepatic steatosis, lobular inflammation, and serum ALT levels, as shown by a clinical trial conducted in NASH patients (Sanyal et al., 2010). Administering pentoxifylline, which is known to decrease oxidative stress and inhibit TNF-α expression, also improved the histological features of NASH in a recent randomized placebo-controlled trial (Zein et al., 2011). In this study, treatment with EGCG lowered the levels of oxidative stress-associated markers such as urinary 8-OHdG and serum d-ROM, whereas elevated the mRNA levels of two antioxidant enzymes, catalase and GPx-1, in the liver of DEN- and HFD-treated SD rats. These findings suggest that EGCG suppressed NAFLD/NASH-related liver tumorigenesis at least partly by reducing systemic and hepatic oxidative stress. Our results are consistent with those of previous studies showing that GTCs can protect against both oxidative stress and the progression of NAFLD to NASH (Park et al., 2011; Ueno et al., 2009; Kuzu et al., 2008).

Besides oxidative stress, chronic inflammation is critically involved in NAFLD/NASH-related liver tumorigenesis (Chiang et al., 2011; Cusi 2012; Siegel and Zhu, 2009; Park et al., 2010). Among the proinflammatory cytokines related to the progression of NASH, TNF-α and IL-6 play a pivotal role in hepatocyte injury and inflammation, which increase HCC risk (Park et al., 2010). Therefore, targeting TNF-α and IL-6 might be an effective method to suppress NAFLD/NASH-related liver tumorigenesis. GTCs are widely recognized to exert cancer-preventive effects partly by inhibiting the expression of TNF-α and IL-6 (Shimizu et al. 2011b; Kochi et al., 2013; Shirakami et al. 2008), indicating that the suppression of inflammation is one of the key mechanisms by which GTCs prevent cancer development. In this study, we found that mRNAs encoding TNF-α, IL-6, and IL-1β were expressed at significantly lower levels in the livers of EGCG-treated rats compared to that in EGCG-untreated rats. Therefore, in agreement with previous reports (Shimizu et al. 2011b; Kochi et al., 2013; Shirakami et al. 2008), the results of this study suggest that EGCG consumption suppressed the development of GST-P-positive foci in DEN- and HFD-treated SD rats by attenuating chronic inflammation.

In addition to reducing oxidative stress and chronic inflammation, both of which are secondary manifestations of NASH, administering EGCG improved hepatic steatosis, a primary manifestation of NASH (Day and James, 1998), decreased serum ALT levels, ameliorated liver fibrosis, and inhibited excessive hepatocyte proliferation in this study. GTCs have been demonstrated to attenuate hepatic fat accumulation in several laboratory animal studies (Kuzu et al., 2008; Kochi et al., 2013; Shimizu et al. 2011b; Park et al., 2011; Ueno et al., 2009);

these reports combined with the findings of this study are of interest because hepatic steatosis *per se* can induce hepatocyte proliferation and hepatic hyperplasia, both of which initiate the hepatic neoplastic process by increasing hepatocyte proliferative activity (Yang et al., 2001). Moreover, hepatic steatosis is critically related to liver fibrosis, which is a strong risk factor for the development of HCC (Powell et al., 2005). Therefore, suppression of hepatic steatosis and fibrosis by EGCG treatment might help to inhibit the progression of NAFLD/NASH-related liver tumorigenesis at an early stage.

Because GST-P-positive foci are generally accepted to be precursors or preneoplastic lesions of HCC in rats (Tsuda et al., 2003; Ando et al., 2007), the rodent model used in this study appears to be well suited for screening reagents that can prevent NAFLD/NASH-related liver tumorigenesis. However, the current study has one limitation that hepatocellular neoplasms, including HCC, did not develop within the experimental period. Because the duration of the experiment (7 weeks) might have been insufficient for the development of hepatic neoplasms, future studies should be conducted using longer-term experiments to confirm that HFD- and DEN-treated SD rats develop hepatocellular neoplasms.

Finally, we emphasize again that targeting metabolic abnormalities, especially oxidative stress and chronic inflammation, might be one of the most practical approaches for treating NAFLD/NASH and preventing NAFLD/NASH-related liver carcinogenesis (Shimizu et al. 2013, 2012). We consider GTCs including EGCG to be potentially effective and key candidates for this purpose, because these agents can target metabolic abnormalities and thus prevent relevant tumorigenesis, as shown by the results of this study and those from previous reports (Shimizu et al. 2011b; Kochi et al., 2013; Shimizu et al. 2008b; Thielecke and Boschmann, 2009; Grove and Lambert, 2010). Recent clinical trials have also demonstrated that GTC supplementation potently prevents the development of both colorectal adenomas and prostate cancers without causing adverse effects (Shimizu et al. 2008a; Bettuzzi et al., 2006). These beneficial effects of GTCs reported in clinical trials strongly encourage the clinical usage of GTCs for treating NAFLD/NASH patients to prevent the metabolic abnormalities, such as steatosis, hyperlipidemia, and hyperinsulinemia, as well as liver carcinogenesis.

Conclusions

In conclusion, administering EGCG effectively suppresses the early stage of hepatocarcinogenesis in our rat model of NAFLD/NASH by attenuating oxidative stress and chronic inflammation. Application of GTCs represents a potential new strategy for preventing the development of hepatic neoplasms in NAFLD/NASH patients.

Methods

Animals and chemicals

Male 7-week-old SD rats were obtained from Japan SLC, Inc. (Shizuoka, Japan) and humanely maintained at Gifu University Life Science Research Center in accordance with the Institutional Animal Care Guidelines. DEN was purchased from Sigma-Aldrich Co. LLC. (St. Louis, MO, USA). HFD-60 (HFD, 506.2 kcal/100 g) with 62.2% of the calories derived from fat was purchased from Oriental Yeast (Tokyo, Japan) (Table 2). EGCG was obtained from Mitsui Norin Co. Ltd. (Tokyo, Japan).

Experimental procedure

The present study was approved by the Experimental Animal Research Committee of Gifu University. After 1-week-acclimatization with regular chow, all rats (n = 19) received a single intraperitoneal injection of DEN (30 mg/kg body weight) and were then randomly divided into 3 groups. Following DEN injection, the rats in Groups 2 and 3 (n = 6 in both groups) were provided tap water containing 0.01% or 0.1% EGCG, respectively, whereas the rats in Group 1 (n = 7) were provided tap water throughout the experiment, which lasted 7 weeks. All rats were fed a pelleted HFD throughout the experiment after DEN injection. At the end of the experiment, the 15-week-old rats were sacrificed by CO_2 asphyxiation and the development of GST-P-positive foci was evaluated. The concentration of EGCG used (0.1%), which was established based on the findings of previous chemopreventive studies

Table 2 Composition and calories of the experimental diet HFD-60

Ingredients	(g/kg diet)
Casein	256.0
Corn starch	160.0
Sucrose	55.0
Dextrose	60.0
Cellulose	66.1
Soybean oil	20.0
Lard	330.0
Vitamin mixture	35.0
Mineral mixture	10.0
Calcium carbonate	1.8
L-cysteine	3.6
Choline bitartrate	2.5
Energy	**(kcal/kg)**
	5062
	(%)
Protein	18.2
Fat	62.2
Carbohydrate	19.6

(Shimizu et al. 2011b; Kochi et al., 2013; Shirakami et al., 2008; 2009), was, in terms of units per body weight, within the physiological range measured in humans after daily intake of GTCs (Wang et al., 1991). Previously, GST-P-positive foci were markedly induced by DEN injection in HFD fed rats, but not in rats fed a normal diet (Wang et al. 2009), therefore we did not use a control group that was fed normal chow diet after DEN injection in the present study.

Histopathological examination and immunohistochemical analyses for GST-P and proliferating cell nuclear antigen (PCNA)

Maximum sagittal sections of 3 liver sublobes (central, lateral, and right-anterior) were used for histopathological examination. Formalin-fixed and paraffin-embedded livers were stained with hematoxylin & eosin (H&E) for conventional histopathology or with Azan stain to detect liver fibrosis. The histological features of the livers were evaluated using the NAFLD activity score (NAS) system (Kleiner et al., 2005), and the development of liver fibrosis was determined as described previously (Kleiner et al., 2005). Immunohistochemistry for GST-P (Ando et al., 2007) and PCNA (Iwasa et al., 2010) was performed using primary antibodies against GST-P (MBL Co. Ltd., Nagoya, Japan) and PCNA (Santa Cruz Biotechnology, Inc., Santa Cruz, CA, USA), respectively. The number of GST-P-positive foci, which was set as 3 or more positive cells (Kochi et al., 2013), was assessed per unit area (per cm^2). In the PCNA-immunostained sections, cells with intensely stained nuclei were considered to be positive for PCNA, and the indices (% PCNA-positive) were determined by counting at least 500 hepatocytes in each section (total of 3000 hepatocytes per rat) (Iwasa et al., 2010).

RNA extraction and quantitative real-time RT-PCR analysis

Total RNA was isolated from the livers of the rats by using RNeasy Mini kit (QIAGEN, Venlo, Netherlands) with on-column DNase I-digestion (Terakura et al., 2012). From 0.2 μg of total RNA, cDNAs were amplified using High-Capacity cDNA Reverse Transcription Kit (Applied Biosystems, Santa Clara, CA, USA) and an automated thermal cycler (Bio-Rad Laboratories, Hercules, CA, USA). Quantitative real-time reverse transcription-PCR (RT-PCR) analysis was performed using specific primers that amplify the TNF-α, IL-1β, IL-6, tissue inhibitor of metalloproteinases (TIMP)-1, TIMP-2, glutathione peroxidase (GPx)-1, catalase, cyclin D1, and glyceraldehyde-3-phosphate dehydrogenase (GAPDH) genes. The sequences of these primers, which were obtained using Primer-BLAST (http://www.ncbi.nlm.nih.gov/tools/primer-blast/), are shown in Table 3. Each sample was analyzed on a LightCycler Nano (Roche Diagnostics, Mannheim, Germany) with FastStart Essential DNA Green Master (Roche Diagnostics). GAPDH amplified in parallel served as the internal control.

Table 3 Primer sequences

Target gene	Direction	Primer sequences (5′-3′)
Catalase	Forward	GCGAATGGAGAGGCAGTGTAC
	Reverse	GAGTGACGTTGTCTTCATTAGCACTG
Cyclin D1	Forward	TTCGTGGCCTCTAAGATGAAGG
	Reverse	TGAGCTTGTTCACCAGAAGCAG
Gapdh	Forward	AGTGCCAGCCTCGTCTCATAG
	Reverse	CCTTGACTGTGCCGTTGAACT
Gpx-1	Forward	GCTCACCCGCTCTTTACCTT
	Reverse	GATGTCGATGGTGCGAAAGC
Il-1β	Forward	AGGCTTCCTTGTGCAAGTGT
	Reverse	TCCTGGGGAAGGCATTAGGA
Il-6	Forward	CACTTCACAAGTCGGAGGCT
	Reverse	AGCACACTAGGTTTGCCGAG
Timp-1	Forward	ACAGCTTTCTGCAACTCGGA
	Reverse	AGTTTGCAAGGGATGGCTGA
Timp-2	Forward	TGGGAACGTGCATTTTGCAG
	Reverse	AAACACTGGTTGGAGGGCAA
Tnf-α	Forward	CCAGACCCTCACACTCAGATCA
	Reverse	TCCGCTTGGTGGTTTGCTA

Clinical chemistry

At sacrifice, the serum levels of ALT were measured using a standard clinical automatic analyzer (Type 7180; Hitachi, Tokyo, Japan).

Hepatic lipid analysis

Total lipids were extracted from approximately 200 mg of liver tissue (frozen at sacrifice) for each rat, and the triglyceride levels were measured using the triglyceride E-test kit (Wako, Osaka, Japan) (Iwasa et al., 2010).

Oxidative stress analysis

Urinary 8-hydroxy-2′-deoxyguanosine (8-OHdG) levels were determined using an ELISA kit (NIKKEN SEIL, Shizuoka, Japan). Serum levels of hydroperoxide, one of the markers for oxidative stress, were determined using the derivatives of reactive oxygen metabolites (d-ROM) test (FREE Carpe Diem; Diacron s.r.l., Grosseto, Italy) (Kochi et al., 2013).

Statistical analysis

All data are expressed as mean ± SD, and one-way analysis of variance (ANOVA) was used for comparisons between groups. If ANOVA indicated significant differences, the Tukey-Kramer test for multiple comparisons was performed to compare the mean values among the groups.

The differences were considered significant when the two-sided *P* value was less than 0.05. All analyses were conducted by the GraphPad InStat software, Version 3.05 (GraphPad Software; San Diego, CA, USA).

Abbreviations

ALT: Alanine aminotransferase; ANOVA: Analysis of variance; Ctrl: Control; DEN: Diethylnitrosamine; d-ROM: Derivatives of reactive oxygen metabolites; EGCG: (−)-epigallocatechin-3-gallate; GAPDH: Glyceraldehyde-3-phosphate dehydrogenase; GPx: Glutathione peroxidase; GST-P: Glutathione *S*-transferase placental form; GTC: Green tea catechin; HCC: Hepatocellular carcinoma; HFD: High-fat diet; IL: Interleukin; NAFLD: Non-alcoholic fatty liver disease; NAS: NAFLD activity score; NASH: Non-alcoholic steatohepatitis; 8-OHdG: 8-hydroxy-2'-deoxyguanosine; RT-PCR: Reverse transcription-PCR; SD: Sprague–Dawley; TG: Triglyceride; TIMP: Tissue inhibitor of metalloproteinase; TNF: Tumor necrosis factor.

Competing interest

The authors declare that they have no competing interest.

Authors' contributions

TS made substantial contributions to conception and carried out the molecular biological studies. YS participated in the design of the study and carried out the molecular biological studies. MS participated in the design of the study and involved in drafting the manuscript and revising. TK carried out the molecular biological studies and made contributions to acquisition of data. TO made contributions to analysis of data. MK made contributions to analysis of data. MS involved in drafting the manuscript and revising. HT involved in drafting the manuscript and revising. TT carried out the pathological studies and performed the statistical analysis. HM made substantial contributions to analysis and interpretation of data and involved in drafting the manuscript and revising. All authors read and approved the final manuscript.

Acknowledgments

This work was supported in part by Grants-in-Aid from the Ministry of Education, Science, Sports and Culture of Japan (No. 22790638 and No.25460988), Grant-in-Aid for the 3rd Term Comprehensive 10-Year Strategy for Cancer Control from the Ministry of Health, Labor and Welfare of Japan, and Takeda Science Foundation.

Author details

[1]Department of Internal Medicine, Gifu University Graduate School of Medicine, Gifu, Japan. [2]Department of Tumor Pathology, Gifu University Graduate School of Medicine, Gifu, Japan. [3]Department of Internal Medicine/Gastroenterology, Gifu University Graduate School of Medicine, 1-1 Yanagido, Gifu 501-1194, Japan.

Received: 26 October 2013 Accepted: 21 December 2013
Published: 27 December 2013

References

Adams LA, Lymp JF, St Sauver J, Sanderson SO, Lindor KD, Feldstein A, Angulo P (2005) The natural history of nonalcoholic fatty liver disease: a population-based cohort study. Gastroenterology 129(1):113–121

Ando N, Shimizu M, Okuno M, Matsushima-Nishiwaki R, Tsurumi H, Tanaka T, Moriwaki H (2007) Expression of retinoid X receptor alpha is decreased in 3'-methyl-4-dimethylaminoazobenzene-induced hepatocellular carcinoma in rats. Oncol Rep 18(4):879–884

Ascha MS, Hanouneh IA, Lopez R, Tamimi TA, Feldstein AF, Zein NN (2010) The incidence and risk factors of hepatocellular carcinoma in patients with nonalcoholic steatohepatitis. Hepatology 51(6):1972–1978. doi:10.1002/hep.23527

Bettuzzi S, Brausi M, Rizzi F, Castagnetti G, Peracchia G, Corti A (2006) Chemoprevention of human prostate cancer by oral administration of green tea catechins in volunteers with high-grade prostate intraepithelial neoplasia: a preliminary report from a one-year proof-of-principle study. Cancer Res 66(2):1234–1240. doi:10.1158/0008-5472.CAN-05-1145

Chiang DJ, Pritchard MT, Nagy LE (2011) Obesity, diabetes mellitus, and liver fibrosis. Am J Physiol Gastrointest Liver Physiol 300(5):G697–G702. doi:10.1152/ajpgi.00426.2010

Cusi K (2012) Role of obesity and lipotoxicity in the development of nonalcoholic steatohepatitis: pathophysiology and clinical implications. Gastroenterology 142(4):711–725. e716. doi:10.1053/j.gastro.2012.02.003

Day CP, James OF (1998) Steatohepatitis: a tale of two "hits"? Gastroenterology 114(4):842–845

Grove KA, Lambert JD (2010) Laboratory, epidemiological, and human intervention studies show that tea (Camellia sinensis) may be useful in the prevention of obesity. J Nutr 140(3):446–453. doi:10.3945/jn.109.115972

Hebbard L, George J (2011) Animal models of nonalcoholic fatty liver disease. Nat Rev Gastroenterol Hepatol 8(1):35–44. doi:10.1038/nrgastro.2010.191

Iwasa J, Shimizu M, Shiraki M, Shirakami Y, Sakai H, Terakura Y, Takai K, Tsurumi H, Tanaka T, Moriwaki H (2010) Dietary supplementation with branched-chain amino acids suppresses diethylnitrosamine-induced liver tumorigenesis in obese and diabetic C57BL/KsJ-db/db mice. Cancer Sci 101(2):460–467. doi:10.1111/j.1349-7006.2009.01402.x

Kleiner DE, Brunt EM, Van Natta M, Behling C, Contos MJ, Cummings OW, Ferrell LD, Liu YC, Torbenson MS, Unalp-Arida A, Yeh M, McCullough AJ, Sanyal AJ (2005) Design and validation of a histological scoring system for nonalcoholic fatty liver disease. Hepatology 41(6):1313–1321. doi:10.1002/hep.20701

Kochi T, Shimizu M, Terakura D, Baba A, Ohno T, Kubota M, Shirakami Y, Tsurumi H, Tanaka T, Moriwaki H (2013) Non-alcoholic steatohepatitis and preneoplastic lesions develop in the liver of obese and hypertensive rats: suppressing effects of EGCG on the development of liver lesions. Cancer Lett. doi:10.1016/j.canlet.2013.08.031

Kuzu N, Bahcecioglu IH, Dagli AF, Ozercan IH, Ustundag B, Sahin K (2008) Epigallocatechin gallate attenuates experimental non-alcoholic steatohepatitis induced by high fat diet. J Gastroenterol Hepatol 23(8 Pt 2):e465–e470. doi:10.1111/j.1440-1746.2007.05052.x

Masterjohn C, Bruno RS (2012) Therapeutic potential of green tea in nonalcoholic fatty liver disease. Nutr Rev 70(1):41–56. doi:10.1111/j.1753-4887.2011.00440.x

Park EJ, Lee JH, Yu GY, He G, Ali SR, Holzer RG, Osterreicher CH, Takahashi H, Karin M (2010) Dietary and genetic obesity promote liver inflammation and tumorigenesis by enhancing IL-6 and TNF expression. Cell 140(2):197–208. doi:10.1016/j.cell.2009.12.052

Park HJ, DiNatale DA, Chung MY, Park YK, Lee JY, Koo SI, O'Connor M, Manautou JE, Bruno RS (2011) Green tea extract attenuates hepatic steatosis by decreasing adipose lipogenesis and enhancing hepatic antioxidant defenses in ob/ob mice. J Nutr Biochem 22(4):393–400. doi:10.1016/j.jnutbio.2010.03.009

Powell EE, Jonsson JR, Clouston AD (2005) Steatosis: co-factor in other liver diseases. Hepatology 42(1):5–13. doi:10.1002/hep.20750

Sanyal AJ, Campbell-Sargent C, Mirshahi F, Rizzo WB, Contos MJ, Sterling RK, Luketic VA, Shiffman ML, Clore JN (2001) Nonalcoholic steatohepatitis: association of insulin resistance and mitochondrial abnormalities. Gastroenterology 120(5):1183–1192. doi:10.1053/gast.2001.23256

Sanyal AJ, Chalasani N, Kowdley KV, McCullough A, Diehl AM, Bass NM, Neuschwander-Tetri BA, Lavine JE, Tonascia J, Unalp A, Van Natta M, Clark J, Brunt EM, Kleiner DE, Hoofnagle JH, Robuck PR (2010) Pioglitazone, vitamin E, or placebo for nonalcoholic steatohepatitis. N Engl J Med 362(18):1675–1685. doi:10.1056/NEJMoa0907929

Schattenberg JM, Galle PR (2010) Animal models of non-alcoholic steatohepatitis: of mice and man. Dig Dis 28(1):247–254. doi:10.1159/000282097

Shimizu M, Fukutomi Y, Ninomiya M, Nagura K, Kato T, Araki H, Suganuma M, Fujiki H, Moriwaki H (2008a) Green tea extracts for the prevention of metachronous colorectal adenomas: a pilot study. Cancer Epidemiol Biomarkers Prev 17(11):3020–3025. doi:10.1158/1055-9965.EPI-08-0528

Shimizu M, Shirakami Y, Sakai H, Adachi S, Hata K, Hirose Y, Tsurumi H, Tanaka T, Moriwaki H (2008b) (−)-Epigallocatechin gallate suppresses azoxymethane-induced colonic premalignant lesions in male C57BL/KsJ-db/db mice. Cancer Prev Res (Phila) 1(4):298–304. doi:10.1158/1940-6207.CAPR-08-0045

Shimizu M, Sakai H, Shirakami Y, Iwasa J, Yasuda Y, Kubota M, Takai K, Tsurumi H, Tanaka T, Moriwaki H (2011a) Acyclic retinoid inhibits diethylnitrosamine-induced liver tumorigenesis in obese and diabetic C57BLKS/J-+(db)/+Lepr(db) mice. Cancer Prev Res (Phila) 4(1):128–136. doi:10.1158/1940-6207.CAPR-10-0163

Shimizu M, Sakai H, Shirakami Y, Yasuda Y, Kubota M, Terakura D, Baba A, Ohno T, Hara Y, Tanaka T, Moriwaki H (2011b) Preventive effects of (−)-epigallocatechin gallate on diethylnitrosamine-induced liver tumorigenesis in obese and diabetic C57BL/KsJ-db/db mice. Cancer Prev Res (Phila) 4(3):396–403. doi:10.1158/1940-6207.CAPR-10-0331

Shimizu M, Yasuda Y, Sakai H, Kubota M, Terakura D, Baba A, Ohno T, Kochi T, Tsurumi H, Tanaka T, Moriwaki H (2011c) Pitavastatin suppresses diethylnitrosamine-induced liver preneoplasms in male C57BL/KsJ-db/db obese mice. BMC Cancer 11(1):281. doi:10.1186/1471-2407-11-281

Shimizu M, Kubota M, Tanaka T, Moriwaki H (2012) Nutraceutical approach for preventing obesity-related colorectal and liver carcinogenesis. Int J Mol Sci 13(1):579–595. doi:10.3390/ijms13010579

Shimizu M, Tanaka T, Moriwaki H (2013) Obesity and hepatocellular carcinoma: targeting obesity-related inflammation for chemoprevention of liver carcinogenesis. Semin Immunopathol 35(2):191–202. doi:10.1007/s00281-012-0336-6

Shirakami Y, Shimizu M, Tsurumi H, Hara Y, Tanaka T, Moriwaki H (2008) EGCG and Polyphenon E attenuate inflammation-related mouse colon carcinogenesis induced by AOM plus DDS. Mol Med Rep 1(3):355–361

Shirakami Y, Shimizu M, Adachi S, Sakai H, Nakagawa T, Yasuda Y, Tsurumi H, Hara Y, Moriwaki H (2009) (−)-Epigallocatechin gallate suppresses the growth of human hepatocellular carcinoma cells by inhibiting activation of the vascular endothelial growth factor-vascular endothelial growth factor receptor axis. Cancer Sci 100(10):1957–1962. doi:10.1111/j.1349-7006.2009.01241.x

Siegel AB, Zhu AX (2009) Metabolic syndrome and hepatocellular carcinoma: two growing epidemics with a potential link. Cancer 115(24):5651–5661. doi:10.1002/cncr.24687

Suzuki Y, Imai K, Takai K, Hanai T, Hayashi H, Naiki T, Nishigaki Y, Tomita E, Shimizu M, Moriwaki H (2013) Hepatocellular carcinoma patients with increased oxidative stress levels are prone to recurrence after curative treatment: a prospective case series study using the d-ROM test. J Cancer Res Clin Oncol 139(5):845–852. doi:10.1007/s00432-013-1389-1

Terakura D, Shimizu M, Iwasa J, Baba A, Kochi T, Ohno T, Kubota M, Shirakami Y, Shiraki M, Takai K, Tsurumi H, Tanaka T, Moriwaki H (2012) Preventive effects of branched-chain amino acid supplementation on the spontaneous development of hepatic preneoplastic lesions in C57BL/KsJ-db/db obese mice. Carcinogenesis 33(12):2499–2506. doi:10.1093/carcin/bgs303

Thielecke F, Boschmann M (2009) The potential role of green tea catechins in the prevention of the metabolic syndrome - a review. Phytochemistry 70(1):11–24. doi:10.1016/j.phytochem.2008.11.011

Tsuda H, Fukushima S, Wanibuchi H, Morimura K, Nakae D, Imaida K, Tatematsu M, Hirose M, Wakabayashi K, Moore MA (2003) Value of GST-P positive preneoplastic hepatic foci in dose–response studies of hepatocarcinogenesis: evidence for practical thresholds with both genotoxic and nongenotoxic carcinogens. A review of recent work. Toxicol Pathol 31(1):80–86

Ueno T, Torimura T, Nakamura T, Sivakumar R, Nakayama H, Otabe S, Yuan X, Yamada K, Hashimoto O, Inoue K, Koga H, Sata M (2009) Epigallocatechin-3-gallate improves nonalcoholic steatohepatitis model mice expressing nuclear steroi regulatory element binding protein-1c in adipose tissue. Int J Mol Med 24(1):17–22

Wang ZY, Agarwal R, Bickers DR, Mukhtar H (1991) Protection against ultraviolet B radiation-induced photocarcinogenesis in hairless mice by green tea polyphenols. Carcinogenesis 12(8):1527–1530

Wang Y, Ausman LM, Greenberg AS, Russell RM, Wang XD (2009) Nonalcoholic steatohepatitis induced by a high-fat diet promotes diethylnitrosamine-initiated early hepatocarcinogenesis in rats. Int J Cancer 124(3):540–546. doi:10.1002/ijc.23995

Wang Y, Ausman LM, Greenberg AS, Russell RM, Wang XD (2010) Dietary lycopene and tomato extract supplementations inhibit nonalcoholic steatohepatitis-promoted hepatocarcinogenesis in rats. Int J Cancer 126(8):1788–1796. doi:10.1002/ijc.24689

Yang S, Lin HZ, Hwang J, Chacko VP, Diehl AM (2001) Hepatic hyperplasia in noncirrhotic fatty livers: is obesity-related hepatic steatosis a premalignant condition? Cancer Res 61(13):5016–5023

Yang CS, Wang X, Lu G, Picinich SC (2009) Cancer prevention by tea: animal studies, molecular mechanisms and human relevance. Nat Rev Cancer 9(6):429–439. doi:10.1038/nrc2641

Zein CO, Yerian LM, Gogate P, Lopez R, Kirwan JP, Feldstein AE, McCullough AJ (2011) Pentoxifylline improves nonalcoholic steatohepatitis: a randomized placebo-controlled trial. Hepatology 54(5):1610–1619. doi:10.1002/hep.24544

doi:10.1186/2193-1801-2-690
Cite this article as: Sumi *et al.*: (−)-Epigallocatechin-3-gallate suppresses hepatic preneoplastic lesions developed in a novel rat model of non-alcoholic steatohepatitis. *SpringerPlus* 2013 2:690.

Oncogene (2013) 32, 2140–2149

www.nature.com/onc

ORIGINAL ARTICLE

FHL1 on chromosome X is a single-hit gastrointestinal tumor-suppressor gene and contributes to the formation of an epigenetic field defect

K Asada[1,7], T Ando[1,2,7], T Niwa[1], S Nanjo[1], N Watanabe[1], E Okochi-Takada[1], T Yoshida[1], K Miyamoto[3], S Enomoto[4], M Ichinose[4], T Tsukamoto[5], S Ito[6], M Tatematsu[5], T Sugiyama[2] and T Ushijima[1]

Tumor-suppressor genes on chromosome X can be inactivated by a single hit, any of the point mutations, chromosomal loss and aberrant DNA methylation. As aberrant DNA methylation can be induced frequently, we here aimed to identify a tumor-suppressor gene on chromosome X inactivated by promoter DNA methylation. Of 69 genes on chromosome X upregulated by treatment of a gastric cancer cell line with a DNA-demethylating agent, 5-aza-2′-deoxycytidine, 11 genes had low or no expression in the cell line and abundant expression in normal gastric mucosae. Among them, *FHL1* was frequently methylation-silenced in gastric and colon cancer cell lines, and methylated in primary gastric (21/80) and colon (5/50) cancers. Knockdown of the endogenous *FHL1* in two cell lines by two kinds of shRNAs significantly increased cell growth *in vitro* and sizes of xenografts in nude mice. Expression of exogenous *FHL1* in a non-expressing cell line significantly reduced its migration, invasion and growth. Notably, a somatic mutation (G642T; Lys214Asn) was identified in one of 144 colon cancer specimens, and the mutant *FHL1* was shown to lack its inhibitory effects on migration, invasion and growth. *FHL1* methylation was associated with *Helicobacter pylori* infection and accumulated in normal-appearing gastric mucosae of gastric cancer patients. These data showed that *FHL1* is a methylation-silenced tumor-suppressor gene on chromosome X in gastrointestinal cancers, and that its silencing contributes to the formation of an epigenetic field for cancerization.

Oncogene (2013) **32,** 2140–2149; doi:10.1038/onc.2012.228; published online 11 June 2012

Keywords: field for cancerization; chromosome X; DNA methylation; gastrointestinal cancer; *Helicobacter pylori*

INTRODUCTION

Inactivation of tumor-suppressor genes is deeply involved in cancer development and progression.[1] The vast majority of tumor-suppressor genes are somatically inactivated by two hits of both alleles by genetic and/or epigenetic mechanisms, such as point mutations, chromosomal deletions and aberrant DNA methylation of promoter CpG islands (CGIs).[2,3] The two-hit theory makes tumor-suppressor genes on chromosome X unique because they can be inactivated by a single hit, and thus are 'risky' genes. So far, three examples have been identified, including *WTX* in Wilms tumors,[4] *FOXP3* in breast and prostate cancers[5,6] and *PHF6* in T-cell acute lymphoblastic leukemia (T-ALL),[7] all of which are inactivated by a point mutation or chromosomal loss.

Among the mechanisms of tumor-suppressor gene inactivation, aberrant DNA methylation can be present not only in tumor tissues but also in normal-appearing tissues, such as non-cancerous tissues of gastric,[8,9] colon,[10] liver,[11] esophageal,[12–14] breast[15] and renal cancer patients.[16] Levels of aberrant DNA methylation in non-cancerous tissues correlate with cancer risk clearly for gastric cancers[8,17] and other cancers, and accumulation of aberrant DNA methylation in a tissue is considered to form an epigenetic field for cancerization (epigenetic field defect).[18] Such association has been analyzed using methylation levels of marker genes, which are methylated in association with various tumor-suppressor genes and show much higher levels, and only a limited number of genes that functionally contribute to the field defect have been identified.

To identify risky genes that contribute to the formation of an epigenetic field defect, we here searched for genes on chromosome X from the 495 genes whose expression was upregulated fourfold or more after treatment with a DNA-demethylating agent, 5-aza-2′-deoxycytidine (5-aza-dC)[19] of a gastric cancer cell line (AGS), which is known to have very frequent methylation of CGIs.[20]

RESULTS

Screening of methylation-silenced genes on chromosome X

Among the 495 genes whose expression was upregulated fourfold or more by treatment of the AGS gastric cancer cell line with 5-aza-dC, 69 genes were located on chromosome X. Among the 69 genes, 11 genes had low expression (signal intensity <200) in non-treated AGS cells and had high expression (signal intensity >500) in a pool of gastric mucosae of three healthy volunteers.

[1]Division of Epigenomics, National Cancer Center Research Institute, Tokyo, Japan; [2]Third Department of Internal Medicine, University of Toyama, Toyama, Japan; [3]Institute for Clinical Research and Department of Surgery, National Hospital Organization Kure Medical Center/Chugoku Cancer Center, Hiroshima, Japan; [4]Second Department of Internal Medicine, Wakayama Medical University, Wakayama, Japan; [5]Division of Oncological Pathology, Aichi Cancer Center Research Institute, Nagoya, Japan and [6]Department of Gastroenterological Surgery, Aichi Cancer Center Hospital, Nagoya, Japan. Correspondence: Dr T Ushijima, Division of Epigenomics, National Cancer Center Research Institute, 5-1-1 Tsukiji, Chuo-ku, Tokyo 104-0045, Japan.
E-mail: tushijim@ncc.go.jp
[7]These authors contributed equally to this work.
Received 20 September 2011; revised 25 April 2012; accepted 4 May 2012; published online 11 June 2012

Genomic structures were analyzed for these 11 genes, and eight of them had CGIs in their promoter regions (Supplementary Table 1). Their mRNA expression levels were confirmed by quantitative reverse transcription–PCR (qRT–PCR) in non-treated AGS cells and gastric epithelial cells obtained by the gland isolation technique, and five (*MAOA, CXorf26, FHL1, SMARCA1* and *MAOB*) had consistent expression in gastric epithelial cells (Supplementary Table 1). Among the five genes, we focused on the *FHL1* gene, because it was reported to be able to inhibit growth, migration, invasion and metastasis of multiple types of cancer cells.[21–26] The other four genes were not reported to be involved in cancer development in the literature.

Promoter methylation and silencing of *FHL1* in gastrointestinal cancer cell lines

DNA methylation status of the *FHL1* promoter region was analyzed using two sets of methylation-specific PCR (MSP) primers designed to cover a region from the transcription start site to 220 bp upstream (Figure 1a). Among the 73 cancer cell lines analyzed (11 gastric, 7 colon, 12 lung, 12 skin, 7 pancreas, 4 esophageal, 4 prostate, 6 breast and 10 ovary cancer cell lines; Supplementary Table 2), *FHL1* was completely methylated (no unmethylated DNA molecules detected) in seven gastric, three colon (Figure 1b) and one lung cancer cell lines. In normal-appearing gastric and colonic mucosae, and peripheral leukocytes of healthy volunteers, *FHL1* was completely unmethylated in males, and partially methylated in females (Figure 1c). The partial methylation in females was considered to reflect methylation of the inactive chromosome X, which is shown later.

The role of the promoter methylation in downregulation of *FHL1* expression was analyzed. First, an association between the methylation and loss of expression was confirmed among the 11 gastric and 7 colon cancer cell lines. *FHL1* was consistently unexpressed in seven gastric and three colon cancer cell lines with its complete methylation (Figures 2a and b), but was expressed in most of the cancer cell lines without methylation, in normal colonic epithelial cells (CRL1790 and CRL1831) and in normal-appearing gastric and colonic mucosae. Second, when promoter methylation was removed by 5-aza-dC treatment of AGS and

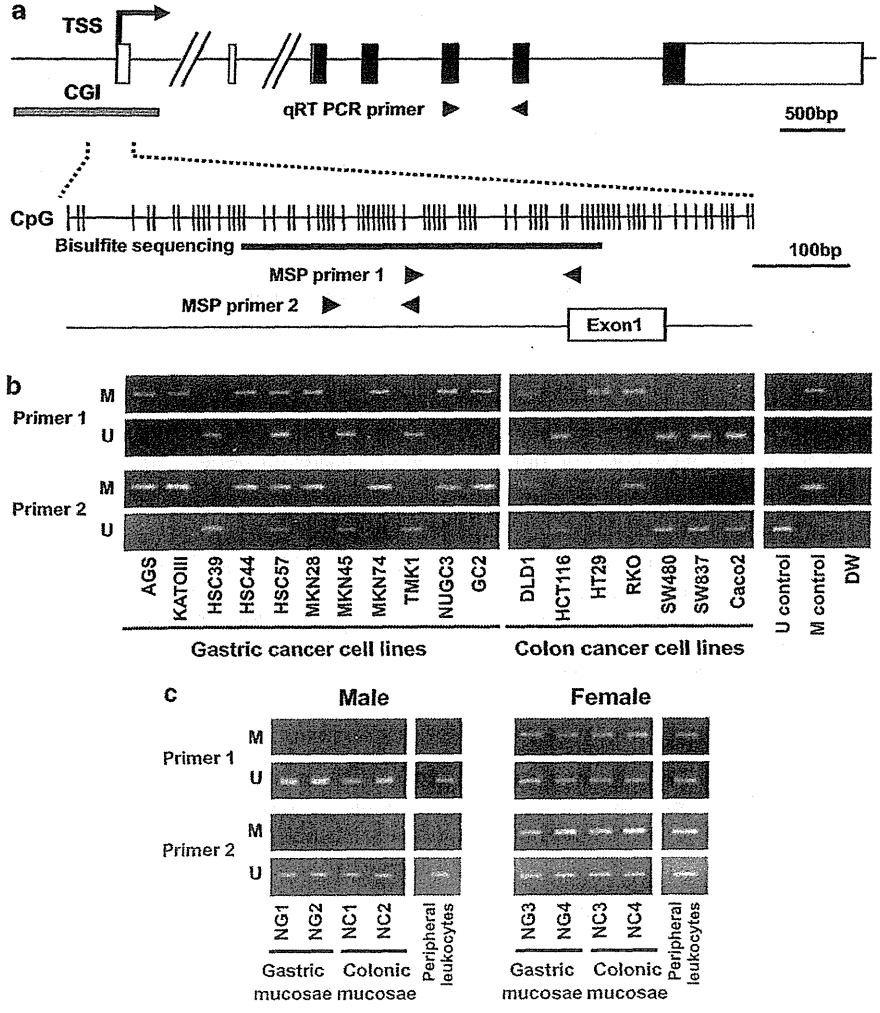

Figure 1. Genomic structure of *FHL1* and its methylation status in cancer cell lines, normal-appearing mucosae and peripheral leukocytes. (a) Genomic structure of *FHL1* and a CpG map of its promoter CGI. Open box, non-coding exon; closed box, coding exon; arrow, transcription start site (TSS); gray box, CGI region; vertical lines, individual CpG sites; arrowheads, primers for qRT-PCR and MSP; and bold line and number, the region and individual CpG sites analyzed by bisulfite sequencing. (b) Promoter methylation of *FHL1* in 11 gastric and seven colon cancer cell lines analyzed by MSP. M and U, primer sets specific to methylated and unmethylated DNA, respectively; U control, fully unmethylated genomic DNA; and M control, fully methylated genomic DNA. *FHL1* was frequently methylated in gastric and colon cancer cell lines. (c) Promoter methylation of *FHL1* in male and female normal-appearing gastric and colonic mucosae and peripheral leukocytes. *FHL1* was completely unmethylated in males and partially methylated in females.

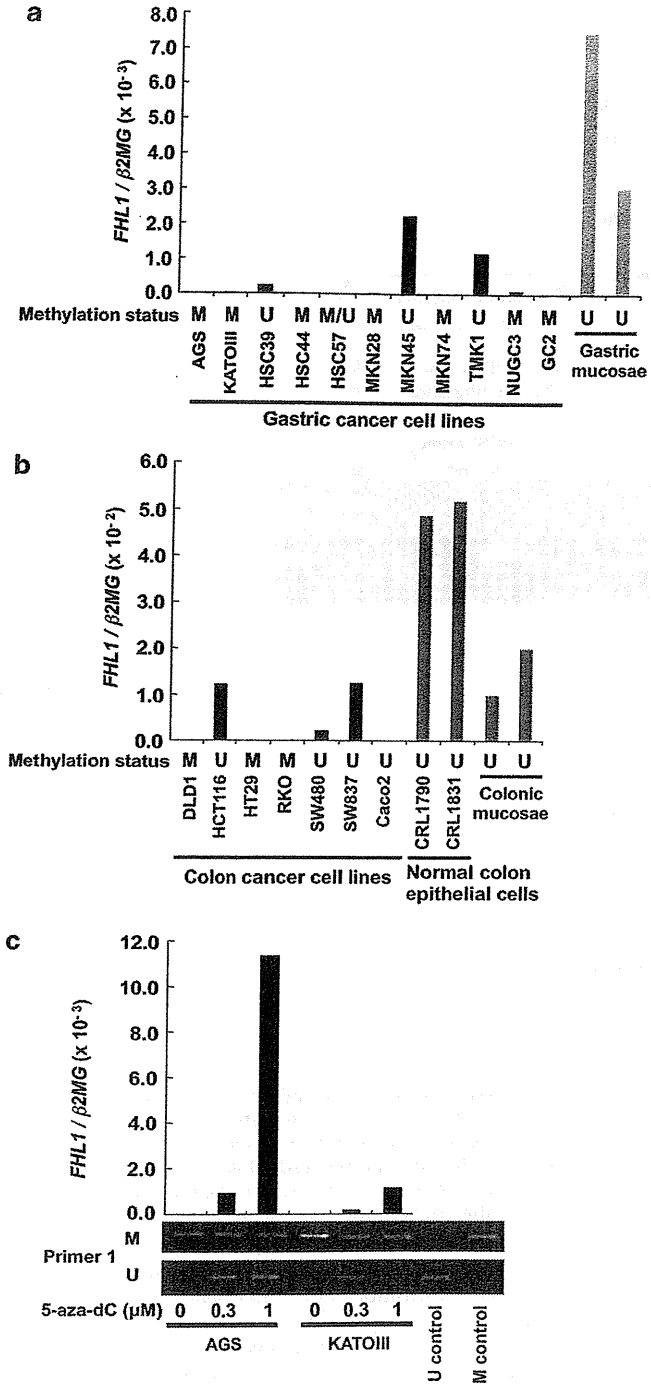

Figure 2. Methylation-silencing of *FHL1* in gastrointestinal cancer cell lines. (a) qRT–PCR of *FHL1* in gastric cancer cell lines and normal-appearing gastric mucosae. Results of MSP in Figure 1b are shown by M, M/U and U. M, only methylated DNA detected; M/U, both methylated and unmethylated DNA detected; and U, only unmethylated DNA detected. *FHL1* was not expressed in cell lines with complete methylation. (b) qRT-PCR of *FHL1* in colon cancer cell lines, normal colonic epithelial cells and normal-appearing colonic mucosae. *FHL1* was not expressed in cell lines with complete methylation. (c) Re-expression and demethylation of *FHL1* after 5-aza-dC treatment of AGS and KATOIII. *FHL1* expression was induced, along with its demethylation, after treatment with 5-aza-dC. U control, fully unmethylated genomic DNA; and M control, fully methylated genomic DNA.

KATOIII gastric cancer cell lines, *FHL1* expression was restored (Figure 2c). These data demonstrated that promoter methylation of *FHL1* caused its silencing.

Methylation of *FHL1* in surgical gastrointestinal cancer specimens

FHL1 methylation in surgical cancer specimens was analyzed by quantitative real-time MSP (qMSP) of 80 gastric and 50 colon cancers derived from male patients (Figure 3a). We adopted a cutoff value of 6%, which was previously determined based on the lowest methylation levels of tumor-suppressor genes in cancer samples,[9,27] and was also used in other researchers' report.[28] *FHL1* was methylated in 21 of the 80 (26%) gastric cancers and 5 of the 50 (10%) colon cancers. The presence of dense methylation of the promoter region was confirmed by bisulfite sequencing, and the fraction of densely methylated DNA molecules was in accordance with the methylation level obtained by qMSP (Figure 3b).

Association between promoter methylation and decreased expression was analyzed in 33 cancer specimens for which RNA was available. The mean *FHL1* expression level of 11 cancers with methylation was significantly lower than that of 22 cancers without methylation ($P = 0.04$) (Figure 3c). Considering that surgical cancer specimens are contaminated with normal cells, the findings here supported that *FHL1* was methylation-silenced also in surgical cancer specimens.

Association between *FHL1* methylation and the CpG island methylator phenotype

Clinicopathological characteristics of cancers with *FHL1* methylation were analyzed in the 80 gastric cancers. *FHL1* methylation was not associated with tumor invasion, lymph node metastasis and histological type (Table 1). In contrast, *FHL1* methylation was associated with the presence of the CGI methylator phenotype (CIMP), 17 of 21 cancers with *FHL1* methylation (81%) and 13 of 59 without being CIMP-positive (22%; $P = 2.9 \times 10^{-6}$). *FHL1* methylation was associated with the presence of Epstein–Barr virus (EBV) infection ($P = 0.02$), but not with *hMLH1* methylation. This suggested that, between the two subtypes of CIMP-positive gastric cancers (those with EBV infection and those with *hMLH1* methylation),[29] *FLH1* methylation was associated with the former.

Growth-suppressive activity of *FHL1*

The effect of the *FHL1* expression loss on cell growth was analyzed by knocking down *FHL1* first *in vitro*. Two *FHL1*-specific shRNAs (sh1and sh2), along with a control shRNA (luciferase-specific shRNA; Luc-sh), were introduced into two cancer cell lines with *FHL1* expression (HCT116 and HSC39). *FHL1* expression was confirmed to be strongly suppressed by sh1 (11.7% of the control cells) and sh2 (14.8%) by qRT–PCR and also by western blot (Figure 4a). *FHL1* knockdown accelerated cell growth in HCT116 cells (sh1, 243% of control cells at 120 h, $P < 0.001$, and sh2, 191%, $P < 0.001$) and in HSC39 cells (sh1, 144% of control cells at 96 h, $P < 0.01$, and sh2, 130%, $P < 0.01$) (Supplementary Figure 1). Then, *in vivo* growth assay using a nude mouse xenograft model showed that HCT116 cells with *FHL1* knockdown formed 2.7-fold larger tumors than control cells (Luc-sh) ($P < 0.001$) (Figure 4b), and that their mean weight was 2.8-fold heavier than that of control cells (Figure 4c). The maintenance of *FHL1* decrease by shRNA was confirmed (Supplementary Figure 2).

The growth-suppressive activity was further analyzed by expressing exogenous *FHL1* in two non-expressing cell lines (AGS and MKN28). By qRT–PCR and western blot, expression levels of the exogenous *FHL1* in AGS and MKN28 were shown to be ~10- and 40-fold, respectively, of those in non-cancerous gastric mucosae (Figures 4d and 5a, and Supplementary Figure 3a). *FHL1* expression reduced the cell growth in AGS (22.2% of control

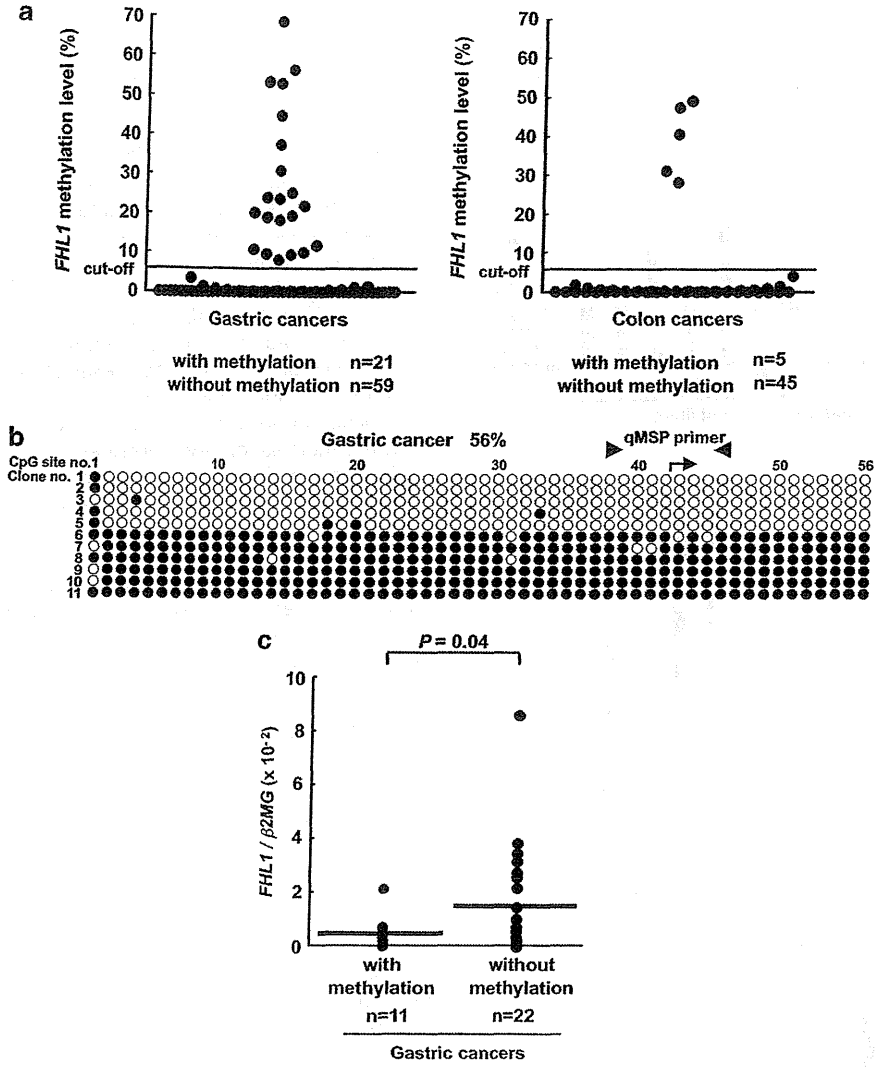

Figure 3. Methylation of *FHL1* in surgical gastrointestinal cancer specimens and its effect on expression. (**a**) Methylation levels in gastric (left) and colon (right) cancers derived from male patients. A horizontal line shows a cutoff value of 6%. *FHL1* was methylated in 21 of 80 primary gastric cancers and 5 of 50 colon cancers, respectively. (**b**) Confirmation of *FHL1* methylation by bisulfite sequencing. Fifty-six CpG sites were analyzed in a gastric cancer with a methylation level of 56%, and six of 11 DNA molecules were densely methylated. Closed circle, methylated CpG site; open circle, unmethylated CpG site; arrowheads, primers for qMSP; and arrow, transcription start site. (**c**) Decreased expression of *FHL1* in gastric cancers with methylation analyzed by qRT–PCR. A horizontal line represents the mean expression level in each group.

cells at 120 h, $P<0.05$; Figures 4d and 5b) but not in MKN28 (Supplementary Figure 3b).

Inhibitory effects of *FHL1* on migration and invasion

To clarify the mechanisms of how *FHL1* works as a tumor-suppressor gene, inhibitory effects of *FHL1* on cell migration and invasion were analyzed in two cell lines (AGS and MKN28). *FHL1* inhibited cell migration both in AGS (26.6% of control cells, $P<0.01$, Figure 5c) and in MKN28 (33.1% of control cells, $P<0.01$, Supplementary Figure 3c). In addition, *FHL1* inhibited cell invasion both in AGS ($P<0.05$, Figure 5d) and in MKN28 ($P<0.05$, Supplementary Figure 3d). In contrast, no induction of apoptosis was observed in AGS by terminal deoxynucleotidyl transferase dUTP nick end labeling assay (Supplementary Figure 4).

An *FHL1* mutation and its loss of function

FHL1 mutations were analyzed by sequencing its seven exons in 58 gastric and 144 colon cancer specimens derived from male patients. A somatic mutation (G642T, Lys214Asn) in exon 6 was identified in a colon cancer (Figure 5e). Also, a synonymous polymorphism (C450T) was observed in two gastric cancers. In the cancer with the G642T mutation, *FHL1* methylation was absent (data not shown), suggesting that either this mutation or promoter methylation was sufficient to inactivate *FHL1*. Further, the effects of the G642T mutation were analyzed by exogenously expressing the mutant and wild-type *FHL1* at similar levels (Figure 5a and Supplementary Figure 3a) in non-expressing AGS and MKN28 cells. The mutant *FHL1* lacked the inhibitory effects on migration and invasion both in AGS (Figures 5c and d) and in MKN28 (Supplementary Figures 3c and d). The mutant *FHL1* also lacked its inhibitory effect on cell growth in AGS (Figure 5b), whereas such effect could not be analyzed in MKN28, whose growth was not suppressed even by wild type *FHL1*. These data indicated that the mutation was a loss-of-function mutation.

FHL1 methylation levels in non-cancerous gastric and colonic mucosae

To analyze the association between *FHL1* methylation and *Helicobacter pylori* (*H. pylori*) infection, and the contribution of